People's Democratic Republic of Algeria
الجمهورية الجزائرية الديمقراطية الشعبية
Ministry of Higher Education and Scientific Research
وزارة التعليم العالي و البحث العلمي

Djilali Bounaama University of Khemis Miliana
Science and Technology Faculty
Department of Material Science

Dissertation

In Fulfilment of the Requirement for the Master's Degree

In Theoretical Physics

Analytical and Numerical Treatment of the Bethe-Bloch Formula with Application in Medicine

Presented by:
CHERIFI Safia

Supervisor :
BENZAID Djelloul

Co-Supervisor :
BENTRIDI Salaheddine

In front of the Jury:

Ms. ZAOUI Sanaa : Chair
Mr. DOUICI Mohamed : Examinator

Class of UDBKM 2023

Dedication

"*I dedicate this work from the depths of my heart to:*
MY DEAR PARENTS
No matter what I do or say, I cannot express enough my respect, eternal love, and consideration for the sacrifices you have made to ensure my education and well-being. I thank you for all the support and love you have shown me since my childhood, and I hope that your blessings will always be with me. May this humble work translate my gratitude and affection.
MY DEAR SIBLINGS
Ali, Wided, Hadjer, Soundous et Salsabil, thank you very much for being always with me and for your moral and financial support. May God keep us for each other.
ALL MY PHYSICS PROFFESSORS
I would like to thank you very much for the quality of the teaching you have given us over the past five years, as well as all your kind treatment and encouragement. I am grateful to have been your student.
MY DEAR FRIENDS
Amina and Rihab, thank you for being by my side over the years, encouraging me, supporting me and for all the good memories you have shared with me.
MY SUPERVISOR AND CO-SUPERVISOR
Mr. Benzaid and Mr. Bentridi, thank you for your efforts in ensuring that this work was completed to a high level.
May God bless you with health, happiness and, above all, success."

- Safia

acknowledgements

First and foremost, I would like to express my deep gratitude to God for granting me the health and willpower to begin and complete this thesis.

I extend my sincere gratitude to my thesis supervisor, Mr. Benzaid, whose exceptional advice, unwavering patience, outstanding diligence and constant availability were invaluable during the research and writing of this thesis.

I would also like to express my deep gratitude to Mr. Bentridi, my co-supervisor, whose invaluable help proved crucial to the successful completion of this work.

I am also grateful to Mr. Bitam for his detailed tutoring on SRIM, which made my work much easier.

Lastly, I would like to express my gratitude to the members of the jury, namely Mr. Douici and Ms. Zaoui, for having kindly agreed to judge my dissertation.

Abstract

In this dissertation, The main objective is to develop a home-made code with FORTRAN to calculate stopping and range of charged particles in matter, in order to compare them with results given by SRIM to see which method provides more accurate and precise outcomes.

A medical application is also explored in the present study by using TRIM sub module (simulate irradiation of a tumour in a living tissue) to highlight the important role of charged particles in cancer and tumour treatment.

Keywords : SRIM, TRIM, Stopping power, Range, Bragg curve, Simulation, Bethe-Bloch formula.

Résumé

Dans ce memoire, l'objectif principale est de développer un code FORTRAN pour calculer le pouvoir d'arrêt et le parcours des particules chargées dans la matière, afin de les comparer aux résultats donnés par SRIM et déterminer quelle méthode offre des résultats plus précis. Une application médicale est également explorée dans la présente étude en utilisant le sous-module TRIM (simulation de l'irradiation d'une tumeur dans un tissu vivant) pour mettre en évidence l'importance des particules chargées dans le traitement du cancer et des tumeurs.

Mots clés : SRIM, TRIM, Pouvoir d'arrêt, Parcours, Courbe de Bragg, Simulation, formule de Bethe-Bloch.

في هذه الأطروحة، يكمن الهدف الرئيسي في تطوير برنامج باستخدام لغة الفورتران لحساب قدرة التوقف ومدى الجسيمات المشحونة في المادة، من أجل مقارنتها بالنتائج المعطاة من قبل برنامج SRIM لرؤية أي الطريقتين توفر نتائج أكثر دقة.

لقد قمنا ايضا بتطبيق في المجال الطبي بواسطة TRIM (محاكاة اشعاع ورم في نسيج حي) لتسليط الضوء على الدور المهم للجسيمات المشحونة في معالجة الاورام و السرطانات.

كلمات مفتاحية :

قدرة التوقف، المدى ،محاكاة TRIM، SRIM، Bethe-Bloch.

Contents

List of Figures

List of Tables

Abbreviations

SRIM *Stopping and Range of Ions in Matter.*

TRIM Transport of Ions in Matter.

FORTRAN *Formula Translation.*

General Introduction

The Bethe-Bloch formula is a theoretical model that describes the mean energy loss of charged particles traversing matter such as electrons, positrons, protons and heavy ions. It was developed by Hans Bethe and Felix Bloch in the 1930s and has been widely used in various fields of physics, such as nuclear physics, particle physics, medical physics, materials science and space science. Nevertheless, it has certain limitations and hypotheses which may not be applicable to all situations and all materials. This formula is not accurate for particles with very low energy or for materials with unusual properties, such as a very high atomic number or density. It also predicts the range of charged particles in matter, which is important for understanding the behaviour of cosmic rays in the Earth's atmosphere and for developing radiation detection technologies. As a general rule, the Bethe-Bloch formula plays a vital role in understanding the how charged particles behave in matter. There are several methods for determining the energy loss and range of charged particles in matter. One of these methods is the SRIM (Stopping and Range of Ions in Matter) simulation code, a Monte Carlo program that uses empirical models and experimental data to simulate the interactions between ions and matter. SRIM is able to provide detailed information on the energy loss, range and damage produced by ions in various materials and geometries.

The main objective of this dissertation is to develop a code with FORTRAN program to determine the energy loss and range of charged particles in order to compare them with the results obtained with SRIM simulation code, and decide which method gives the most accurate and significant results. We have taken the interaction of protons and alpha particles with aluminium as an example. We will also do an application in medical physics (simulation of the irradiation of a tumour in the thyroid gland) to highlight the important role of charged particles in cancer and tumour treatments.

The present dissertation is composed of four chapters:

- **Chapter 1 : Theory of Ionizing Radiation Interaction with Matter**

  The first one is dedicated to the theory of interaction of ionizing radiations with matter including charged, neutral and electromagnetic ones.

- **Chapter 2 :Interaction of charged particles with matter**

  In the second chapter, we will discuss the interactions of charged particles with matter in depth, presenting the interactions of electrons, positrons, and heavy particles with matter by citing their sources of interactions, their passage through matter, and their stopping power. We will also discuss the range and Bragg curve.

- **Chapter 3 :Analytical and numerical calculations**

  In the third chapter we will focus on comparing the results taken from the classical Bethe-Bloch formula implemented in FORTRAN with those from the SRIM simulation code. stopping power curves, ranges and Bragg curves of alpha particles and protons in aluminium are taken as an example in our study.

- **Chapter 4 :Simulation of Stopping Power and Range into Living Tissues**

  In the fourth chapter, we will do an application in medicine by using TRIM simulation code to treat the irradiation of a tumour that's located in the thyroid gland.

- **Conclusion** Finally, this work ends with a conclusion.

Chapter 1

Theory of Ionizing Radiation Interaction with Matter

1.1 Introduction

The theory of ionizing radiation interaction with matter is a basic concept in the field of radiation physics and radiation protection. It describes how ionizing radiation interacts with matter when passing through it. The study of the interaction of ionizing radiation with matter dates back to the late $19^{th}$and early 20^{th} centuries, when scientists first discovered that some types of radiation could ionise the atoms and molecules of materials. At the end of the 19^{th}century, Wilhelm Röntgen discovered $X - rays$, which turned out to be a type of electromagnetic radiation. Soon scientists realised that $X - rays$ were able to penetrate matter and cause ionisation to atoms and molecules they pass through. Early in the $1900s$, the discovery of radioactivity by Marie Curie and her husband Pierre Curie was made. Radioactivity is the spontaneous emission of ionizing radiation by certain atoms. The discovery of radioactivity resulted in the study of the properties and interactions of several types of ionizing radiation, particularly α, β particles and γ rays. The Danish physicist Niels Bohr developed a model of the atom in 1913 which explained how electrons interact with the nucleus. This model was used to explain how ionizing radiation interacts with matter, since it showed that electrons could be ejected from atoms when bombarded by radiation. Over the years, scientists have pursued the study of the interaction of ionizing radiation with matter, with more sophisticated models and experimental techniques being developed to understand the complex processes involved. Nowadays, the study of ionizing radiation plays a key role in different areas including medical imaging, radiotherapy, nuclear energy and industrial radiation protection and much more. Throughout this chapter, we will indicate how ionizing radiation interacts with matter. We will explore the various sources of interaction and radiation, including electromagnetic radiation and neutral particles. Additionally, we will provide an overview of the interaction of charged particles with matter.

1.2 Radiation and particle interaction

To detect radiation we should make it interact with the material of the detector and then study the changes that happened in the system configuration [**1**]. The results of the detection operation are converted into signals. The types and energy of primary particles are important factors in the interaction processes [**2**]. Instruments for radiation detection develop with the availability of new technologies, as a result, more advanced devices will be provided to users. For example, we find complex, large and advanced instruments in use for many applications like nuclear medicine and space physics [**2**]. The energy-loss process operates by the interaction of the electric field associated with the moving charge and the one generated by the electronic structure of detecting media, it allows the dissipation of energy inside the detecting medium itself [**2**].

1.3 Types of interaction

It is well established that the nature is governed by four fundamental interactions.

1.3.1 Strong interaction:

The gluon mediates the strong interaction, particles interacting with this type are known as hadrons (Hadrons are a class of subatomic particles that are composed of quarks, which are elementary particles) that are classified into two main types:

Hadrons with half-integer spin values(fermions like protons and neutrons).
Mesons with integer spin values(bosons like pions).

These types of interaction provides the necessary binding forces to hold together nucleus. Its relative strength of interaction at distances about $10^{-18} cm$ is 1[**2**].

1.3.2 Electromagnetic interaction:

The photon mediates the electromagnetic interaction, usually, it is responsible for almost all non-nuclear interactions in physics beyond the gravitational attraction.The theory of quantum electrodynamics allows extremely exact calculations of particles. Its relative strength of interaction at distance of 10^-18cm cm is: 10^{-2}[**2**].

1.3.3 Weak interaction:

W and Z(bosons) mediate the weak interaction, this type is responsible for some processes like $\beta-$ decays in nuclear physics. Its relative strength of interaction at distance of 10^-18 cm is: 10^-5[**2**].

1.3.4 Gravitational interaction:

It's an interaction that includes massive bodies at very large distances,but, at short distances, it has a negligible effect in particle-particle interaction. Its relative strength of interaction at distance of 10^-18 cm is: 10^-39[**2**].
It's evident that part of interactions are unified, for example, electromagnetic and weak interactions have been unified in the electroweak theory[**2**].

1.4 Properties and sources of radiation

The term radiation describes the transportation of mass and energy through space. It plays a dominant role in our lives in various fields. Radiation has several benefits like medical diagnosis tics and also damages like atomic explosions and radiation exposure; it has unlimited potential, it can open up doors to many developments if we use it properly.

1.4.1 Sources of radiation

There are two main sources of radiation: natural and man-made.

Natural sources:

Because of their intensity relatively very low, natural sources are, in general, not dangerous to our bodies, like Cosmic, terrestrial and internal radiations. However, there are some potentially risk materials like radon because they are capable to delivering integrated doses [**1**].

Man-made sources:

After the discovery of radiations, scientists worked on developing sources that produce them in controlled laboratory environments. Usually, they give one type of radiation and they are made for a particular purpose (for example: medical $X - ray$ machines, nuclear medicines, particle accelerators, lasers). However, there are also some products that emit radiation, for example: television, phones,building materials and laptop...etc [**1**]. The table below shows some of the radioactive elements that are produced very frequently [**1**].

Element	Common Isotopes (Decay Mode)	Common Use
Cobalt	${}^{60}_{27}Co(\beta)$	Surgical instrument sterilization
Technetium	${}^{99}_{43}Tc(\beta)$	Medical diagnostics
Iodine	${}^{123}_{53}I(\beta, EC), {}^{129}_{53}I(\beta), {}^{131}_{53}I(\beta)$	Medical diagnostics
Xenon	${}^{133}_{54}Xe(\beta)$	Medical diagnostics
Caesium	${}^{137}_{35}Cs(\beta)$	Treat cancers
Iridium	${}^{192}_{77}Ir(\beta)$	Integrity check of welds and parts
Polonium	${}^{210}_{84}Po(\alpha)$	Static charge reduction in photographic films
Thorium	${}^{299}_{90}Th(\alpha)$	Extend life of fluorescent lights
Plutonium	${}^{238}_{94}Pu(\alpha)$	α-particle source
Americium	${}^{241}_{95}Am(\alpha)$	Smoke detectors

Table 1.1: Common Radioactive Isotopes of Elements

1.4.2 Types of ionizing radiation

In this section we will give some important radiations that are very used in our day life.

Alpha radiation

Or helium, ${}^{4}_{2}He$, is one of the most known nuclear particles. It is composed of four nucleons, two protons and two neutrons. Alpha particle is not very penetrating and can be stopped by a sheet of paper or the outer layer of human skin.

Beta radiation

Beta radiation is made up of fast moving electrons emitted from the nucleus of an atom. It is negatively charged and can pass through materials including wood and plastic, although it can be stopped by aluminium or thin metal sheets.

Gamma radiation

Gamma radiation is a highly radioactive form of electromagnetic radiation emitted by the nucleus of an atom. It is extremely penetrating and can penetrate thick layers of concrete, steel and other materials.

Neutron radiation

Neutron radiation is free neutrons that are emitted during nuclear fission and radioactive decay. It is highly penetrating and can pass through most materials, but can be attenuated by materials rich in hydrogen atoms.

X-ray radiation

X-rays are a form of electromagnetic radiation with shorter wavelengths than gamma rays. It can penetrate soft tissue but is absorbed by denser materials such as bone.

Ultraviolet radiation

Ultraviolet (UV) radiation is a form of electromagnetic radiation with shorter wavelengths than visible light. It can lead to sunburn and is a known carcinogen.

1.5 Radioactivity

It's a natural process in which some atomic nucleus disintegrate spontaneously by losing energy in the form of radiation (it is also called radioactive decay). It occurs because of unstable isotopes that tend to transform into a more stable state. There are three distinct types of radioactivity: α-rays; β-rays and γ-rays.

α-rays: They are made up of alpha particles which are equivalent to helium atom, these rays are absorbed by thin layers of matter easily [**4**].

β-rays: there are two types: β^+ and β^-; they are composed of particles with negative charge and projected with high velocity.

γ-rays: they are a form of electromagnetic radiation which are emitted from an excited nucleus and they have a very penetrating character.

Decay equation:

The activity of radioisotope source is considered to be its decay rate and is defined by the first principle law of radioactive decay [**1**], which is:

$$N = N_0 e^{-\lambda t} \tag{1.1}$$

where λ is the decay constant and N is the number of radioactive nuclei and N_0 is the number of radioactive atoms in the sample at $t = 0$.

Activity of a source of radiation:

Activity is the decay rate A, it is defined by the formula:

$$A = A_0 \exp(-\lambda t) \tag{1.2}$$

where $A_0 = \lambda N_0$ is the initial activity.

Another parameter, which is widely cited and used, is the half-life. It is defined as the time needed for the decay of half of the nuclei in a sample. It is written as:

$$T_{\frac{1}{2}} = 0.693\tau \tag{1.3}$$

Where $\tau = \frac{1}{\lambda}$ which is the mean life.

1.6 Electromagnetic radiation interaction in matter

Within matter, any kind of moving charged particle loses energy. The heavier particles than electrons will lose energy, principally by the excitation and ionization of atoms of the medium, nearby their trajectory. As the energy increases some of the scattered electrons may be escaping from the (thin) absorber or detection medium. Therefore, the deposited energy may be less then the energy lost by a charged particle. In the case of heavy ions, which have a velocity of the order of the Bohr orbital velocity of electrons in the hydrogen atom, the energy loss from collisions with the target nuclei is no more negligible. Electrons (and positrons) can also lose energy by radiating photons. The most significant processes for photon absorption in matter are photoelectric production, Compton production and electron-positron pair production [**2**]. The energy of the electromagnetic radiation is always defined by the Planck relation:

$$E_r = h\nu = h\frac{c}{\lambda} = \hbar \tag{1.4}$$

Where $h = 6.6210^{-27} erg.s = 6.6210^{-34} Js$

1.6.1 Passage of ionizing particles through matter

Ionising particles, including alpha particles, beta particles and gamma rays, has enough energy to ionise or break down atoms or molecules when passing through matter. However, the degree of ionization varies depending on the type of particle, its energy and the density of the material through which it passes.
Alpha particles have significant mass and a positive charge, making them highly ionizing, but they have a short range, usually a few centimetres in the air. In contrast, beta particles have a smaller mass and a negative charge, so they are less ionizing than alpha particles, but they have a longer range in air and are able to penetrate deeper into materials. Gamma rays, which are high-energy photons, have neither mass nor charge, but are highly penetrating and can travel long distances through air and matter.
When ionizing particles pass through matter, they interact with the atoms and molecules of the matter, resulting in ionization and excitation. Such interactions can lead to the creation of free electrons, which can cause further ionization in a process known as secondary ionization. This can create a cascade of ionization events, which can have harmful effects on living tissue.
The degree of ionization provided by ionizing particles is measured in terms of radiation dose, which is the amount of energy deposited by the particles in a given amount of material. This dose depends on the type and energy of the particles, the type and density of the material and the distance from the radiation source. The effects of radiation exposure on living tissue depend on the dose and type of radiation and can range from mild to severe, including DNA damage, cell death and cancer.
Charged particles passing through matter lose their kinetic energy by electromagnetic

interactions that dominate and consist of the excitation and ionization of atoms in their path. This process is generally referred to as collision's loss process or collision process. Later collision processes, mediated by the electromagnetic field combined with the entering charged particles and targets in the medium (i.e. bound electrons and nuclei) result in the formation of the primary ionization. The resulting fast electrons produced by the ionization processes are called γ rays. If they are energetic enough, these electrons will also excite and ionize atoms. Therefore, a secondary process of ionization will happen. Nevertheless, the energy deposited per unit path within the medium is generally less than the energy lost from collisions, because faster γ rays may be fully absorbed away from the location where they were generated or escape from the medium. In addition, deviations in the direction of arrival are generally small, but become significant in the final phase of total absorption processes[**2**].

1.6.2 Gamma rays interaction

For gamma rays, we have three main types that play an important role in radiation measurement: photoelectric absorption, Compton scattering and pair production. All these processes are responsible for the partial or complete transfer of the gamma ray energy into electronic energy. They lead to sudden and abrupt changes in the gamma-ray history, in that the photon disappears entirely or is scattered at a large angle[**3**].

Photoelectric absorption

In this process, the incident photon is absorbed during a collision with a bound electron (binding energy E_b) which is released and carries part of the energy E_γ of the photon under kinetic form. The photo-electron is appearing with an energy defined by:

$$E_e = h\nu - E_b \tag{1.5}$$

Compton scattering

In Compton scattering, the incident gamma-ray photon is deviated by an angle from its original direction. The photon transfers some of its energy to the electron (supposed to be initially at rest), which is then known as a recoil electron. Since all scattering angles are possible, the energy that is transferred to the electron can be varied from zero to a significant fraction of the energy of the gamma ray. The expression relating the energy transfer and the scattering angle for any particular interaction can be obtained by simultaneously writing equations for the conservation of energy and momentum[**3**].

$$E'_\gamma = \frac{E_\gamma}{1 + \frac{E_\gamma}{m_0 c^2}(1 - \cos\theta)} \tag{1.6}$$

The Compton scattering probability per absorber atom depends on the number of electrons that are available as scattering targets and thus increases linearly with Z [**3**].

Pair production

If the energy of gamma rays exceeds twice the rest mass energy of an electron ($1.02MeV$), the pair production process is energetically possible. In fact, the probability of this interaction is very small until the gamma-ray energy is close to several MeV and, consequently, the pair production is mainly limited to high energy gamma-rays. Within the interaction, the gamma photon disappears and is exchanged for an electron-positron pair. All the surplus energy transported by the photon above the $1.02MeV$ needed to create the pair is converted into kinetic energy which is shared by the positron and the electron. Since the positron then annihilates after slowing down in the absorbing medium, two annihilation photons are normally produced as side products of the interaction. There is no simple expression for the pair production probability per nucleus, however its magnitude varies approximately as the square of the atomic number. The importance of pair production increases strongly with energy[**3**].

$$\gamma_{incident} + M_{atrest} \rightarrow M + e^- + e^+ \tag{1.7}$$

1.6.3 Gamma-ray attenuation

Attenuation coefficient

Each of the interaction processes eliminates the gamma photon of the beam by either absorption or scattering away from the detector direction and can be characterized by a fixed probability of occurrence per unit path length in the absorber. The summation of these probabilities is merely the probability, per unit path length, that the gamma photon is removed from the beam; it's called the linear attenuation coefficient[**3**]:

$$\mu = \tau(photoelectric) + \sigma(compton) + k(pairproduction) \tag{1.8}$$

I is the number of transmitted photons and it's given in terms of I_0 (the number without an absorber) as:

$$\frac{I}{I_0} = \exp(-\mu t) \tag{1.9}$$

λ is the mean free path of gamma ray photons which is defined as the average distance travelled in the absorber before reaching an interaction, it is the inverse of the linear attenuation coefficient.

$$\lambda = \frac{1}{\mu} \tag{1.10}$$

1.7 Interaction of charged particles with matter

Charged particle interaction with matter is a fundamental process in physics. Whenever charged particles, e.g. electrons, protons or ions, travel through matter or interact with it, a number of phenomena occur. The nature of these interactions depends on the particle's type and energy, as well as the properties of the matter they encounter. Here are a few important interactions:

- Ionization.
- Excitation.
- Nuclear reactions.
- Scattering.
- Radiation production.
- Bremsstrahlung.
- Cherenkov Radiation.

1.8 Interaction of Neutral Particles with Matter

Neutral particles, such as neutrons and neutrinos, are able to interact with matter in different ways according to their energy and type. The following are some ways in which neutral particles can interact with matter:

1.8.1 Neutrons

Neutrons are neutral particles, they do not interact with materials through electromagnetic interaction, but they must approach very close to the nuclei to make a strong nuclear interaction. The results are generally charged particles and electromagnetic radiation. In this case, according to their energy, they can interact with the nuclei in the following way:

Elastic scattering The main mode of interaction of neutrons with atomic nuclei is elastic scattering. During this process, the target nucleus stays in the same state after the interaction. The reaction is written $A(n,n)A$ or

$$n + X_p^{n+p} \rightarrow n + X_p^{n+p} \tag{1.11}$$

Inelastic Scattering Contrary to elastic scattering, inelastic scattering will leave the target nucleus in a state of excitation. The reaction is expressed as $A(n,n)A^*$ or

$$n + X_p^{n+p} \rightarrow n + [X_p^{n+p}]^* \tag{1.12}$$

In a such kind of process, the incoming neutron is absorbed by the nucleus, creating a composed nucleus. The composed nucleus is unstable and quickly emits a neutron of lower kinetic energy. Because it still has a surplus of energy, it undergoes one or more γ decays to return to the ground state.

Transmutation Neutrons of all energies are able to produce transmutations. A transmutation is a reaction in which one element is transformed into another[**1**]. For example:

$${}_0^1n +_5^{10} B \rightarrow_5^7 Li +_2^4 \alpha \tag{1.13}$$

Radiative Capture Radiative capture is an extremely common reaction in which neutrons are involved. In this reaction, a nucleus absorbs the neutron and changes to an excited state. In order to come back to the stable state, the nucleus emits γ rays. No transmutation occurs in this case, however the isotopic form of the element changes because of the increase in the number of neutrons[**1**]. The reaction is represented by $A(n,\gamma)A+1$ or

$$^{1}_{0}n +^{n+p}_{p} X \rightarrow^{n+p+1}_{p} X + \gamma \tag{1.14}$$

Spallation Spallation means the fragmentation of a nucleus into many parts when a neutron of high energy collides with it. This process is important only for neutrons with energy above about $100MeV$[**1**].

Fission During this process, a heavy nucleus, like $uranium - 235$, captures a slow neutron, causing it to enter an excited state. The nucleus then splits into fragments after a brief delay. Many neutrons and $\gamma - ray$ photons are emitted during this process as well. The fission of $uranium - 235$ may be written as follows

$$^{1}_{0}n +^{235}_{92} U \rightarrow^{139}_{39} I +^{95}_{53} Y + 2^{1}_{0}n + \gamma \tag{1.15}$$

The fission process is the thermal energy source that is produced in nuclear reactors. The core of a nuclear reactor is a managed environment in which neutrons are permitted to produce the fission chain reaction. In this the neutrons emitted by the fissioning nucleus produce further fissions, which produce even more neutrons. Thus, the fission started by a couple of neutrons rapidly spreads to the entire fissile material. a few neutrons rapidly spreads to the entire fission material. The huge number of fission fragments generated in this way rapidly lose their energy in the material because of their large mass. This energy is released as heat, which is the main thermal energy source in a nuclear reactor. The thermal energy is subsequently transformed into electrical energy by other processes [**1**].

Passage of Neutrons through Matter

The electromagnetic interactions with the atoms of the material do not reduce the energy of neutrons. They can therefore penetrate more deeply into the material than charged particles. This higher ability to penetrate is quite problematic when it comes to developing effective radiation shields around neutron sources,however, deeper penetration also has its advantages. For example, we can use a neutron beam for non-destructive testing of materials. The neutron beam passing through a material undergoes an exponential attenuation[**1**]. The neutron beam intensity at a distance x from the origin can therefore be determined from

$$I = I_0 \exp(-\mu_n x) \tag{1.16}$$

Where μ_n is the attenuation coefficient of neutrons, it is usually given in inverse length dimensions and depends on the type of material and the energy of the neutrons.
The mean free path is defined by

$$\lambda_n = \frac{1}{\mu_n} \tag{1.17}$$

We can also write the attenuation coefficient in total nuclear cross-section terms σ_t, as

$$\mu_n = N\sigma_t = \frac{N_A\rho}{A}\sigma_t \tag{1.18}$$

Where $N = \dfrac{N_A\rho}{A}$ which is the number density of nuclei in the material,N_A is the Avogadro's number, ρ is the weight density of the material and A A is its atomic weight.
We can use the equation(1.36) to determine experimentally the attenuation coefficient of an elementary isotope as we can write μ_n as

$$\mu_n = \frac{1}{x}\ln(\frac{I_0}{I}) \tag{1.19}$$

1.8.2 Photons

A photon is defined as a quantum of electromagnetic energy and considered as a fundamental particle in the standard model of particle physics. As the photon moves through a medium, it decelerates due to the interaction with the medium and acquires an effective mass. However, in a vacuum, it is considered to be mass-less. Photons are not just visible light. In fact, light covers a very narrow region of their full energy spectrum. Similarly, the light we see as visible light is not really considered to be composed of individual photons, but instead a superposition of a number of photons. Photons are involved in all types of electromagnetic interactions[**1**].
Photons are emitted from various sources in the universe, each with its own unique electromagnetic spectrum.

Passage of photons through matter

As photons, which are particles of light, pass through matter, they can either be absorbed, scattered or transmitted. Once a photon is absorbed, the resulting energy is transferred to the matter it encounters. Matter can then be excited, causing chemical reactions or changes in physical state such as fusion or vaporisation. As scattered photons collide with atoms or molecules in matter, they change direction. This can happen in a number of ways, including elastic scattering, where the photon simply changes direction without losing energy, or inelastic scattering, where the photon transfers some of its energy to the matter it encounters. Transmission happens when photons pass through matter without being absorbed or scattered. For this to happen, the photons must have the right amount of energy to pass through the different layers or obstacles in the material. In certain cases, light can be refracted (bent) as it passes through a surface or medium, resulting in interesting optical effects such as the bending of light in a prism. All in all, the behaviour of light when passing through matter is a complex interaction between the properties of matter and those of the photons themselves.
At any point in a material, the decrease in intensity of a photon beam per unit length of material has been found to depend on the intensity at that point[**1**], namely

$$\frac{dI}{dx} \propto -I \Longrightarrow \frac{dI}{dx} = -\mu_t I \tag{1.20}$$

where dI is the change in intensity when the beam passes through the thickness dx; μ_t is the total linear attenuation coefficient. Integrating the above equation gives

$$I = I_0 \exp(-\mu_t x) \tag{1.21}$$

where I_0 is the intensity of the photon beam just before it enters the material and I is its intensity at a depth x. By analogy with the half-life and mean life of radioisotopes, the mean free path λ_m and the half thickness $x_{1/2}$ were defined for the attenuation of the photon beam in materials.

$$\lambda_m = \frac{1}{\mu_t} \tag{1.22}$$

$$x_{1/2} = \frac{\ln(2)}{\mu_t} \tag{1.23}$$

The mass attenuation coefficient is defined by

$$\mu_m = \frac{\mu_t}{\rho} \tag{1.24}$$

Here ρ is the density of the material.
Just like the mean free path, we can also define the specific mean free path using the mass attenuation coefficient like

$$\lambda_p = \frac{1}{\mu_m} \tag{1.25}$$

We can express the total linear attenuation coefficient μ_t in terms of total cross section σ_t as

$$\mu_t = \sigma_t N = \sigma_t \frac{\rho N_A}{A} \tag{1.26}$$

And also, we can write the total mass attenuation coefficient in terms of the total cross section as

$$\mu_m = \sigma_t \frac{N_A}{A} \tag{1.27}$$

The attenuation coefficient is typically measured in units of inverse length and represents the fraction of photons that are absorbed or scattered per unit length of the material.

1.9 Conclusion

In summary, the theory of the interaction of ionizing radiation with matter refers to the study of the way in which radiation interacts with matter, resulting in ionization and energy transfer that can have harmful effects on living organisms and materials. It is an important field for radiation protection and medical imaging, and also for nuclear energy and radiation therapy. The theory involves understanding the properties of radiation, the type and composition of the matter with which it interacts, and the mechanisms by which ionization and energy transfer occur. This knowledge is essential for developing effective radiation protection strategies and optimising medical treatments using radiation.

Chapter 2

Interaction of Heavy Charged Particles with Matter

sectionIntroduction The interaction of charged particles with matter is used to describe the interactions between charged particles (like ions, electrons or positrons) and materials with which they come in contact. For decades, the interaction of charged particles with matter has been studied. Scientists started to study the behaviour of charged particles, like electrons, as they pass through a material in the $19th$ century. In 1897, J.J. Thomson conducted experiments on the interaction of electrons with matter. He noticed that electrons were deflected as they passed through thin sheets of metal and concluded that the electrons must be interacting with the atoms in the material. Early in the $20th$ century, researchers started to study the interaction of charged particles with gases. Ernest Rutherford's experiments proved that positively charged atomic nuclei exist and resulted in the development of the concept of atomic structure. During the $1930s$, physicists began exploring the interaction of charged particles with magnetic fields. Back in the $1950s$, some researchers looked at the interaction of charged particles with living organisms; they found that charged particles could damage living tissue, resulting in the development of radiation therapy for the treatment of cancer. Nowadays, the interaction of charged particles with matter is always an important area of research, with applications ranging from medical imaging to the study of fundamental particles. In all, the study of charged particles had a significant effect on our understanding of the nature of matter and energy. In this chapter, we will see how electrons and charged particles interact with matter, what their stopping powers are, their sources of interaction and their ranges.

2.1 Interaction of charged particles with matter

Heavy charged particles are subatomic particles that carry a significant amount of electric charge and have a relatively large mass. These particles include protons, alpha particles, and heavier ions such as carbon, nitrogen, and oxygen ions interact strongly with other matter, and can cause significant damage to biological tissue when they collide with it. They are commonly used in radiation therapy for cancer treatment, as they can target tumour cells more precisely than other forms of radiation.

2.1.1 Heavy charged particle sources

Heavy nuclei are energetically unstable and therefore do not permit spontaneous emission of alpha particles. The probability of decay is governed by the mechanism of barrier penetration which is described in most nuclear physics texts, and the half-life of useful sources varies from a few days to several thousand years [**3**]. Schematically, the disintegration process is written as follows:

$$^{A}_{Z}X \rightarrow ^{A-4}_{Z-2} Y +^{4}_{2} \alpha \tag{2.1}$$

At each distinct transition from the initial nucleus to the final nucleus, a fixed energy difference or Q-value characterizes the disintegration. The alpha particle and the recoil nucleus share this energy uniquely, so that the **alpha particle** appears with the same energy given by $Q(A-4)/A$. There exist many practical cases where only one such transition is involved and thus the alpha particles are emitted with a unique energy. It is no coincidence that most alpha particles are limited in energy to a value between 4 and 6 MeV. The energy of alpha particles is very strongly correlated with the half-life of the parent isotope, and the highest energies are the ones with the shortest half-life [**3**].
Above about $6.5MeV$, the half-life would be expected to be shorter than a few days, so the usefulness of the source is very limited. In contrast, if the energy falls below $4MeV$, the probability of penetrating the barrier becomes very low and the half-life of the isotope is very large. If the half-life is excessively long, the achievable specific activity in a practical sample of the material gets very low and the source is not interesting because its intensity is too low [**3**].
Since the alpha particles lose energy in materials at a rapid rate, their sources that must be nearly mono-energetic have to be prepared in very thin layers. Typical sources are covered with a metal foil or other material to contain the radioactive material, which also must be kept very thin to preserve the original energy and the mono-energetic nature of the alpha emission [**3**].
The only spontaneous source of energetic heavy charged particles with a mass greater than that of the alpha particle is the **fission process**. Thus, fission fragments are used extensively in the calibration and testing of detectors intended for general application to the measurement of heavy ions. In principle, all heavy nuclei are unstable in the face of spontaneous fission into two lighter fragments. However, for all nuclei, except the extremely heavy ones, the process is inhibited by the large potential barrier that needs to be overcome during the deformation of the nucleus from its initial quasi-spherical form. Spontaneous fission is not a meaningful process, except for certain transuranic isotopes of very high mass number. The most common example is ^{25}Cf, which undergoes spontaneous fission with a half-life (if it were the only decay process) of 85 years. Two fission fragments are formed from each fission and, by conservation of momentum, are emitted in opposite directions[**3**].
Rutherford scattering, which was first discovered by Lord Rutherford, refers to the elastic scattering of a heavy charged particle (like an α particle) from a nucleus. In his well-known scattering experiment, a thin sheet of gold was bombarded with α particles and Rutherford studied how many of them were deflected from their original direction of motion. He noticed that most of the α particles passed through the sheet without being deflected, while a very small number were deflected at very large angles. This experiment showed that most of the space in the atom is empty and that the positive charge is

concentrated in a small space, which today we call the nucleus. This pioneering work by Rutherford changed forever the way atoms are viewed[**1**].

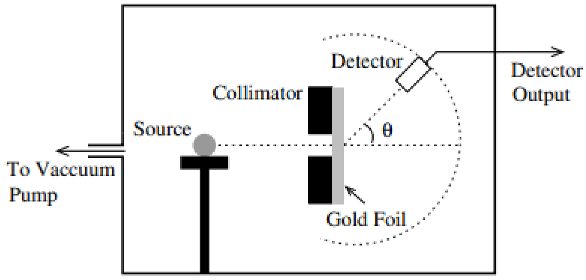

Figure 2.1: A simple setup to determine the angular distribution of Rutherford scattering.

2.2 Passage of charged particles through matter

Charged particles interact in different ways in matter:

2.2.1 Ionization

When charged particles pass through matter, they can strip electrons from atoms and molecules, leading to ionisation. This process usually results in energy deposition and can significantly affect the properties of the medium.

2.2.2 Excitation

Rather than removing electrons, charged particles can also deposit energy by exciting them to higher energy levels. Such excited atoms or molecules can then emit radiation when they return to their ground state.

2.2.3 Nuclear reactions

Depending on the energy of the charged particle, it can induce nuclear reactions in the target material. For instance, a high-energy proton hitting a nucleus can lead to its fission or fusion, releasing other particles and energy.

2.2.4 Bremsstrahlung

As charged particles decelerate in matter, they emit radiation that is called bremsstrahlung. This phenomenon can be important in high energy physics experiments, where it may be desirable to minimise these effects[**3**].

Cherenkov radiation

As charged particles pass through a medium at a speed greater than the speed of light in that medium, they can emit Cherenkov radiation. This is a characteristic blue glow that can be observed in nuclear reactors or high energy physics experiments[**3**].
In general, the interactions of charged particles with matter are complex and depend on many factors including the energy, charge and mass of the particle, as well as the properties of the target material. The ability to understand these interactions is crucial in many fields, including radiation protection, medical physics and particle physics.
The coulomb force due to the charge of the incident particle and the charge of the electrons of the slowing medium is responsible for the slowing down. By slowing down, we mean the gradual decrease of the charged particle, heavy charged particles interact with the matter through coulomb interaction leading to their gradual slowing down during a large number of shocks.

2.2.5 Stopping power for charged particles

The Bethe-Bloch formula is used to describe the rate of energy loss of charged particles when they pass through a material. A history of the Bethe-Bloch formula dates back to the discovery of the electron by J.J. Thomson in 1897. This discovery resulted in the development of the first particle accelerator in 1929, which permitted scientists to study the properties of subatomic particles and their interactions with matter. Back in 1930, quantum mechanics was used by Hans Bethe to derive an equation for the energy loss of fast electrons in matter. This is known as the Bethe equation and was subsequently extended by Bethe and Bloch to other charged particles, such as protons and alpha particles. The Bethe-Bloch formula considers the interactions between charged particles and the atomic electrons of the material they pass through. It predicts that the energy loss of charged particles increases with the density of the material and the square of the charge of the particle. It further indicates that the energy loss is inversely proportional to the square of the particle's velocity. However, there are many important applications of the Bethe-Bloch formula in areas including particle physics, radiation therapy and radiation protection. It is used for predicting the energy loss of charged particles in a variety of materials, and to help design and optimise particle accelerators and radiation detectors. This formula has both classic and relativistic cases.

Relativistic case

The relativistic Bethe-Bloch formula describes the energy loss of a charged particle travelling through a material at relativistic speeds.
Note: The complete derivation of the Bethe-Bloch equation is a complex mathematical process that requires a deep understanding of particle physics and electromagnetic interactions. The following version gives a general overview of the steps involved.

The relativistic Bethe-Bloch equation is defined as[**3**]:

$$S(E) = -\frac{dE}{dx} = \frac{4\pi e^4 z^2 nZ}{m_e v^2}\{\ln(\frac{2m_e v^2}{I_m}) - \ln(1-\beta^2) - \beta^2 - \delta - \frac{2c_k}{Z}\} \quad (2.2)$$

Where dE/dx is the rate of energy loss; e is the electron charge; z is the atomic number of the charged particle; n is the atomic density; Z is the atomic number of the material; m_e is the electron's mass; v is the velocity of charged particle; I_m is the mean ionization potential; $\beta = \frac{v}{c}$ is the velocity of the particle relative to the speed of light and δ is a correction term for the density effect.

The relativistic Bethe-Bloch formula is more precise for high energy particles than the classical formula. The density correction term takes into account the increase in the Coulomb field spreading of the nucleus at high energy.

Classic case, low energies

At low energy, the relativistic Bethe-Bloch formula describes the energy loss of a charged particle travelling through a material at non-relativistic speeds. In this case, we have ($v \ll c$);

$$S(E) = -\frac{dE}{dx} = \frac{4\pi e^4 z^2 nZ}{m_e v^2}\ln(\frac{2m_e v^2}{I_m}) \quad (2.3)$$

A variety of electronic and nuclear mechanisms exist by which charged particles can interact with particles in the medium. Nevertheless, the net result of all these interactions is a reduction in the energy of the particles as they pass through the medium. Although the underlying interaction mechanisms are relatively complicated, the rate of this energy loss can be predicted quite accurately, fortunately, by a number of semi-empirical relationships developed to date [**1**].

The rate at which a charged particle loses energy when passing through a material depends on the nature of the incident and target particles. In the literature, this amount is generally known as the stopping power of the material. It is important to note that stopping power is not the energy loss per unit time, but instead the energy that a charged particle loses per unit length of the material that it passes through. In general, all charged particles can interact electronically, nuclearly or gravitationally with the particles of the matter through which they pass. However, the gravitational interaction is too weak to be significant and is generally ignored. Therefore, the total stopping power is simply the sum of the stopping powers due to the electronic and nuclear interactions[**1**].

$$S_{total} = -\frac{dE}{dx} = S_{electronic} + S_{nuclear} \quad (2.4)$$

In most cases, the nuclear component of the stopping power could be ignored as well, since it is usually only a fraction of the total stopping power. For particles as electrons, this statement is still valid since they remain completely unaffected by the strong nuclear force. For heavy positive charges, such as α particles, this statement is valid only if the energy of the particle is not high enough for it to penetrate so deeply into the atom that the short-range nuclear forces of the nuclear particles become appreciable. Therefore, the stopping power can be written as a function of the electronic component only.

$$-\frac{dE}{dx} \approx S_{electronic} \quad (2.5)$$

The earliest successful attempt to derive a relation for the energy loss experienced by an ion moving through the electromagnetic field of an electron has been made by Neil Bohr. He argued that such an expression could be obtained by just considering the pulses delivered by the ion to the electron as it passes through its electromagnetic field[**1**]. This reflection resulted in the following relation:

$$[-\frac{dE}{dx}]_{Bohr} = \frac{4\pi q^2 e^4 N_e}{m_e v^2} \ln[\frac{\gamma^2 m_e v^3 f(Z)}{qe^2}] \tag{2.6}$$

Where:
e is the unit electron charge,
m_e is the mass of electron,
N_e is the electron number density,
q is the charge of the ion,
v is the velocity of the ion,
$f(Z)$ is a function of the atomic number Z of the material,
γ is the relativistic factor given by $(1 - v^2/c^2)^{-\frac{1}{2}}$.
Later on, Bethe and Bloch derived an alternative expression for stopping power based on quantum mechanics.

$$[-\frac{dE}{dx}]_{Bethe-Bloch} = \frac{4\pi N_A r_e^2 m_e c^2 \rho Z q^2}{A\beta^2}[\ln(\frac{W_{max}}{I}) - \beta^2] \tag{2.7}$$

Where
$N_A = 6.02210^{23} mole^{-1}$ is s the Avogadro's number;
$r_e = 2.81810^{-15} m$ is the classical radius of the electron;
$m_e = 9.10910^{-31} kg$ is the rest mass of the electron;
q is the electrical charge of the ion in units of unit electrical charge;
ρ is the density of the medium;
A is the mass number of the medium;
I is the ionization potential of the medium;
β is a correction factor. It is generally calculated from the relation: $\beta = [1 - \frac{E_0}{E_0 + E/A_i}]^{\frac{1}{2}}$ where $E_0 = 931.5 MeV$ is the rest mass energy per nucleon and E is the energy of the incident particle having mass number A_i;
W_{max} is the maximum energy transferred in the encounter.It can be calculated from: $W_{max} = 2m_e c^2 \beta^2/(1 - \beta^2)$.
The factor $4\pi N_A r_e^2 m_e c^2$ is constant and can thus be permanently substituted in the previous formula, which then becomes:

$$[-\frac{dE}{dx}]_{Bethe-Bloch} = \frac{0.30548 \rho Z q^2}{A\beta^2}[\ln(\frac{W_{max}}{I}) - \beta^2] MeV cm^{-1} \tag{2.8}$$

There are two factors that become significant at very high and moderately low energies that have been corrected in this equation. The first is the shielding of distant electrons due to the polarization of electrons by the electric field of the moving ion. This effect depends on the electron density and increases in importance as the energy of the incident particle increases. The second correction factor is applied at lower energies and depends on the orbital velocities of the electrons. These two correction terms are subtractive and usually represented by the symbols δ and C respectively [**1**]. So, after applying these corrections, the stopping power formula becomes:

$$[-\frac{dE}{dx}]_{Bethe-Bloch} = \frac{4\pi N_A r_e^2 m_e c^2 \rho Z q^2}{A\beta^2}[\ln(\frac{W_{max}}{I}) - \beta^2 - \frac{\delta}{2} - \frac{C}{Z}] \tag{2.9}$$

Instead, the Bethe-Bloch formula could also be written in terms of mass stopping power, which is just the stopping power divided by the density of the medium.

$$[-\frac{1}{\rho}\frac{dE}{dx}]_{Bethe-Bloch} = \frac{4\pi N_A r_e^2 m_e c^2 Z q^2}{A\beta^2}[\ln(\frac{W_{max}}{I}) - \beta^2 - \frac{\delta}{2} - \frac{C}{Z}] \tag{2.10}$$

Note that the above expression for mass stopping power concerns a medium with a single atomic number and is therefore only valid for a pure element [**1**].

2.3 Bragg Curve

The Bethe-Bloch formulas for charged particle stopping power are implicitly dependent on the energy of the particle through factors including β and W_{max}. When a heavy charged particle moves through matter, it loses energy and, as a result, its stopping power changes. Since stopping power measures the efficiency of a particle to cause ionization, the ionization capacity of the particle changes as it moves through matter. In order to understand this dependence, lets plot the Beth-Bloch formula for α particles as a function of their residual energy. By residual energy, we mean the instantaneous energy of the particle retained by it when it passes through the material. To simplify, we will group all terms that are constant for a particular material [**empty citation**].

$$[-\frac{dE}{dc}]_{Bethe-Bloch} = \frac{K}{\beta^2}[\ln(\frac{W_{max}}{10^{-4}}) - \beta^2] MeV cm^{-1} \tag{2.11}$$

Where: $K = 030548\rho Z q^2/A$ is a constant for a given material and $I = 10^{-4} MeV$; this value is typical of low Z materials.

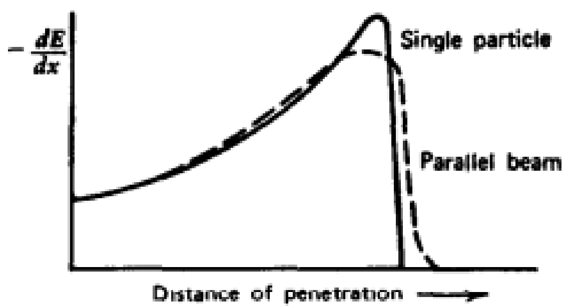

Figure 2.2: Example of Bragg curve for alpha particle

2.4 Range

It is quite tempting trying to calculate the range in a medium by integrating the stopping power over the whole energy spectrum of the incident particles, for example,

$$R(T) = \int_0^t \left[-\frac{dE}{dx}\right]^{-1} dE \tag{2.12}$$

Because of multiple Coulomb scattering, a charged particle's trajectory in a medium is not a straight line. Instead, the particle moves in small straight line segments. This means that the range of a particle beam shows statistical fluctuations around a mean value. By analogy with the phenomenon of energy dispersion, this fluctuation is called range dispersion [**3**].

A number of both empirical and semi-empirical formulas have been suggested to calculate the range of α particles in air. For example[**1**]:

$$R_\alpha^{air}[cm] = 0.56 E_\alpha For E_\alpha < 4MeV \tag{2.13}$$

$$R_\alpha^{air}[cm] = 1.24 E_\alpha - 2.62 For 4MeV \leq E_\alpha < 8MeV \tag{2.14}$$

Various theoretical and experimental studies have been conducted on the variation of proton range as a function of energy in several materials. These studies have resulted in the development of specific empirical relationships for the material studied and in the energy range used in the experiment [**1**]. The range of protons with energy Ep in air can be calculated as follows:

$$R_p^{air}[m] = [\frac{E_p}{9.3}]^{1.8} for E_p < 200MeV \tag{2.15}$$

2.5 Conclusion

To conclude, there are various effects that can result when charged particles interact with matter, depending on the characteristics of the particles and the material with which they interact. As charged particles pass through matter, they can result in ionization, excitation, and radiation damage, which can lead to both beneficial and harmful effects. Charged particle behaviour can be studied with a variety of techniques, including particle detectors and imaging systems. The comprehension of the interaction of charged particles with matter is crucial for many fields, including medicine, nuclear energy and space research. However, further research and advances in this area are needed to improve our understanding and to develop new technologies that can be of benefit to society.

Chapter 3

Analytical and Numerical Calculation

3.1 Introduction

The upcoming chapter will focus on developing FORTRAN programs to determine a charged particle's stopping power and range using Bethe's formula. We'll analyse our results and compare them to those obtained using the *SRIM* code, a highly-regarded particle stopping calculation tool. The objective of this chapter is to understand the features and behaviour of charged particles within matter. To achieve this, we will take the examples of protons and alpha particles within aluminium. Subsequently, we will create Bragg curves using TRIM simulation code to further comprehend the particles' behaviour.

3.2 SRIM code, Stopping and Range of Ions in Matter

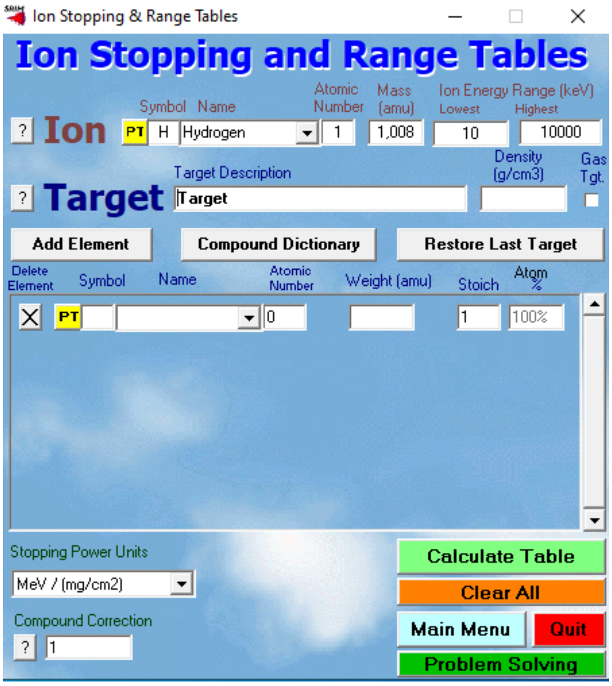

Figure 3.1: SRIM calculation code

SRIM (The Stopping and Range of Ions in Matter) is a group of programs which calculate the stopping and range of ions into matter using a quantum mechanical treatment of ion-atom collisions (assuming a moving atom as an "ion", and all target atoms as "atoms"). This calculation is made very efficient by the use of statistical algorithms which allow the ion to make jumps between calculated collisions and then averaging the collision results over the intervening gap. During the collisions, the ion and atom have a screened Coulomb collision, including exchange and correlation interactions between the overlapping electron shells. The ion has long range interactions creating electron excitation and plasmon within the target. These are described by including a description of the target's collective electronic structure and inter-atomic bond structure when the calculation is setup (tables of nominal values are supplied). The charge state of the ion within the target is described using the concept of effective charge, which includes a velocity dependent charge state and long range screening due to the collective electron sea of the target[7].

3.3 FORTRAN Program

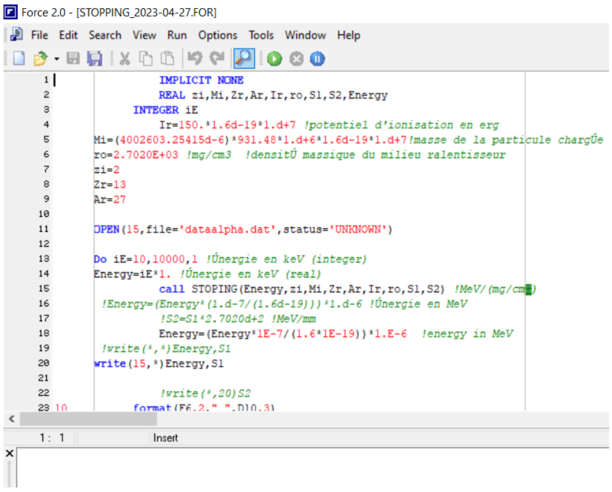

Figure 3.2: FORTRAN code

FORTRAN (Formula Translation) is a programming language widely used in engineering and scientific applications. It was one of the first high-level programming languages developed in the 1950*s*. It is still used today, although more recent languages have gained in popularity.

A FORTRAN program is a set of instructions written in the FORTRAN programming language. These programs are used to solve mathematical and scientific problems by specifying a sequence of computational steps. Typically, FORTRAN programs involve the declaration of variables, the definition of equations and mathematical formulas, and the implementation of control structures such as loops and conditional statements.

In our work, we developed a FORTRAN code for the classical Bethe-Bloch formula using Simpson's method. We used FORTRAN to translate our algorithm into code, declaring the necessary variables, writing loops for integration using Simpson's method, and using the equations of the Bethe-Bloch formula to perform the appropriate calculations.

3.4 Analytical calculations of Bethe-Bloch formula

We're going to establish, in an elementary context, the expression for the energy loss per unit length of a charged particle in a material.

The energy loss, ΔE incurred by the incident particle during an elementary interaction with an electron is linked to the kinetic energy acquired by this electron, E_e, by the conservation of energy: ΔE= -E_e, it's a very low energy, so that we can write[**10**]:

$$E_e = \frac{(p_2^{'})^2}{2m_e} = \frac{(-\Delta p)^2}{2m_e} = \frac{(\Delta p)^2}{2m_e} \tag{3.1}$$

Where, m_e is the mass of the electron, p is its impulse and Δp is the impulse transfer of the incident particle.

$p_e^{'} = -\Delta p$ means that the atomic electrons were initially at rest. In fact, in the large number of these interactions over the thickness dx, the incident particle encounters as many bound electrons with an impulse, p_e, directed in one direction as in the opposite direction, so that we have $< p_e >= 0$[**10**].
Thus, to evaluate ΔE, we need to calculate $|\Delta p| = 2p\sin\theta/2$. Let's first consider the case of an interaction occurring at impact parameter b and note that, for high energies, scattering occurs mainly at very low angles[**10**], we obtain:

$$|\Delta p| = 2p\sin\theta/2 \simeq 2mv\frac{ze^2}{mbv^2} \simeq \frac{2ze^2}{bv} \tag{3.2}$$

Where v is the particle's velocity. We conclude:

$$(\Delta E)_b = -E_e = -\frac{|\Delta p|^2}{2m_e} = -\frac{2z^2e^4}{m_e v^2 b^2} \tag{3.3}$$

The probability of a collision occurring at this value b is proportional to $2\pi bdb$, so that the number of such collisions occurring in thickness dx is given by: $n_b = (2\pi \text{ b db})(dx.\aleph)$, where $\aleph$ is the number of diffusers per cm^3. Since the energy of the incident particles is much greater than the binding energy of any electron, we assume in the following case that there is no need to distinguish between the Z electrons of each atom, and we therefore write: $\aleph = N.Z$, where N is the number of atoms per cm^3[**10**]. Therefore, the energy loss becomes:

$$dE_b = n_b(\Delta E)_b = -\frac{4\pi z^2 NZ}{m_e v^2}\frac{db}{b}dx \tag{3.4}$$

Integrating all conceivable impact parameters between two limit values b_{min} and b_{max}, we obtain:

$$-\frac{dE}{dx} = \frac{4\pi z^2 e^4 NZ}{m_e v^2}\log\frac{b_{max}}{b_{min}} \tag{3.5}$$

Where:

$$b_{max} = \frac{\hbar\nu}{I\sqrt{1-\beta^2}} \tag{3.6}$$

$$b_{min} = \frac{\hbar\sqrt{1-\beta^2}}{2m_e v} \tag{3.7}$$

Finally, we obtain[**10**]:

$$-\frac{dE}{dx} = \frac{4\pi z^2 e^4 NZ}{m_e v^2}\log\left[\frac{2m_e v^2}{I\sqrt{1-\beta^2}}\right] \tag{3.8}$$

3.5 Stopping power

Stopping power refers to the ability of a material or substance to decrease or absorb the energy of charged particles that pass through it, often expressed in terms of energy loss per unit path length. It is dependent on the type of charged particle or projectile (usually an ionized atom), the target material or host (phase, density, and temperature conditions), and, all else being equal, the kinetic energy or, in other words, the velocity of the charged particle. There is an additional dependence in crystalline materials on the relative orientation of the crystal with respect to the principal direction of the projectile velocity. This dependence on orientation is only natural if one considers stopping power as an effect resulting from interactions occurring at the atomic scale, including a set of sequential or simultaneous many-body Coulomb collisions. At the microscopic level, this energy loss is the effect of a retarding force due to collisions with the particles that make up the material[**5**].

3.5.1 Stopping power of α-particles

The amount of energy lost by alpha particles as they pass through a material is represented by the alpha particle stopping power curve. The stopping power is low at first as the alpha particle travels through the lower density outer regions of the material. As it penetrates deeper into the material, the stopping power increases. This is because the alpha particle encounters more electrons, thus losing more energy. At some point, the stopping power attains a maximum. Following the peak, the stopping power decreases as more electrons are encountered and the alpha particle penetrates deeper into the material[**1**].
The formula used here is:

$$S(E) = -\frac{dE}{dx} = \frac{4\pi e^4 z^2 n Z}{m_e v^2}\ln(\frac{2m_e v^2}{I_m}) \tag{3.9}$$

We have selected alpha particles within an energy range of 10 keV to 10 MeV.

With SRIM

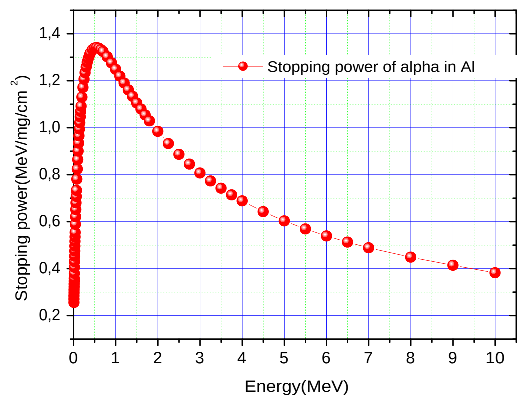

Figure 3.3: Stopping power of alpha in Al using SRIM

This graph shows the stopping power of alpha particles in aluminium using the SRIM simulation code. We note that at the beginning of the curve, when the alpha energy is low, the stopping power is very high and reaches its maximum at 0.55 MeV. In the interval [0.55,2] MeV, the stopping power begins to decrease, but stays high. Above 4 MeV, the stopping power decreases again but very slowly.

With our FORTRAN code

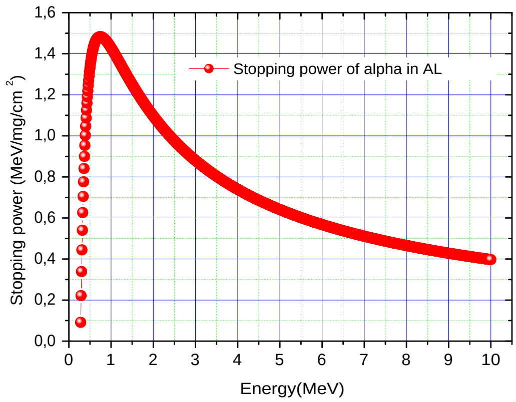

Figure 3.4: Stopping power of alpha in Al

This graph shows the stopping power of alpha particles in aluminium using the classical Bethe-Bloch formula developed by the program FORTRAN. At the beginning of the curve, the stopping power is very high and reaches the Bragg peak at 0.74 MeV, then starts to decrease as the energy of alpha particles increases.

3.5.2 Stopping power of protons

The proton stopping power curve in aluminium illustrates the relationship between proton energy and the amount of energy it loses as it passes through the aluminium. This stopping power is low at high energies and the proton loses little energy as it passes through the material. When the energy of the proton decreases, its stopping power increases and the proton loses more energy per unit distance travelled.
The formula used here is:

$$S(E) = -\frac{dE}{dx} = \frac{4\pi e^4 z^2 n Z}{m_e v^2} \ln(\frac{2m_e v^2}{I_m}) \tag{3.10}$$

We have selected protons within an energy range of 10 keV to 10 MeV.

With SRIM

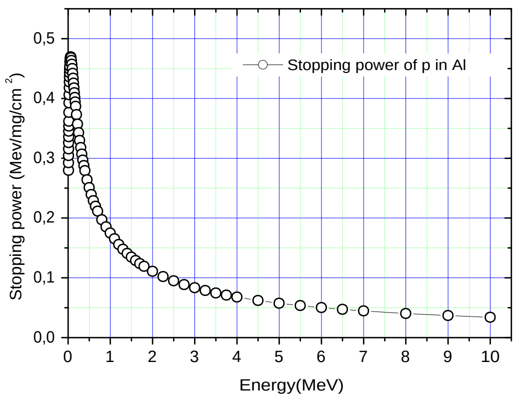

Figure 3.5: Stopping power of proton in Al

We can clearly observe on this curve that at 0.07 MeV , the stopping power is the highest. In the [0,4] MeV range, the stopping power is very high and then starts to decrease as the energy increases.

With our FORTRAN code

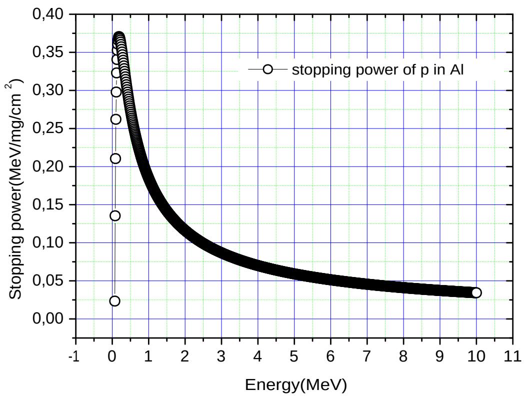

Figure 3.6: Stopping power of proton in Al

Here, in the stopping power curve plotted by our code developed using FORTRAN program, we can see that the peak occurs at 0.1 MeV which means that at this point, the proton loses the maximum of its energy. In the [0.1,4] MeV range, the stopping power is still high, although as the energy of the protons increases, the stopping power decreases.

Comparison between stopping power curves of proton and alpha in aluminium:

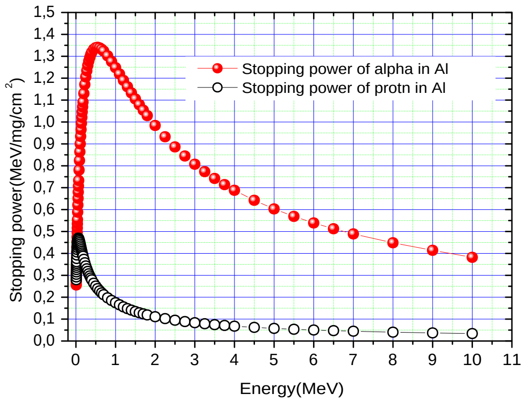

Figure 3.7: Stopping power of alpha and proton in Al

The stopping power of a particle is a measure of the energy loss per unit distance travelled by the particle. Due to differences in their interactions with matter, the stopping power curve of alpha and proton in aluminium is different.
Alpha particles are much heavier and have a higher charge than protons. Thus they interact more powerfully with the electrons and nuclei of the target material. This leads to a higher energy loss rate. Alpha particles also undergo more frequent and stronger Coulomb interactions with the nuclei of the target, increasing their energy loss.
At the same time, protons are lighter and have a lower charge, which means that their interactions with matter are less strong than those of alpha particles. They have a less pronounced stopping power curve than alpha particles. Protons interact mainly with electrons in the target material by ionisation and excitation and, as they penetrate deeper, they undergo diffusion with nuclei.
In short, the alpha particle stopping power curve in aluminium shows a higher energy loss because of their stronger interaction with the target material. Protons, in contrary, have a lower energy loss because of their weaker interactions with the target material.

Comparison between the stopping power curves generated by SRIM and those calculated using our FORTRAN code

The stopping power curves created by SRIM and the ones calculated using the FORTRAN code have a rather similar shape, both exhibiting an almost linear increase of the stopping power with decreasing energy up to a minimum value. Nevertheless, we can notice some differences in these curves.

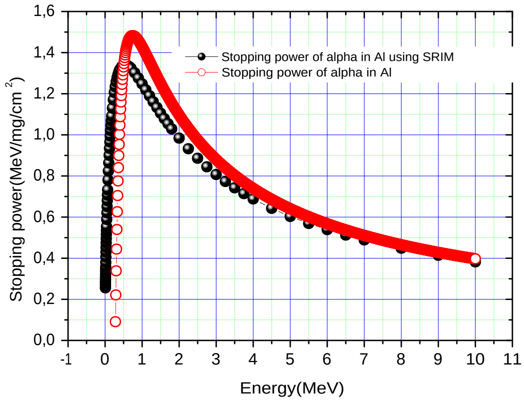

Figure 3.8: Stopping power of alpha in Al

Based on the illustration, it can be seen that the stopping power curve of α particles produced by SRIM is slightly lower than those calculated using our FORTRAN code. This difference is more pronounced at lower energy levels. In addition, there is a slight divergence in the maximum stopping power between the two curves. In SRIM, the peak is lower and occurs at lower energy (0.55 MeV) than in FORTRAN code which is higher (0.74 MeV). However, at low energies the shape of the curve is somehow different, in the SRIM curve the minimum stopping power is at 0.01 MeV which is almost equal to 0 MeV, whereas, in the other curve the minimum stopping power is at 0.31 MeV. However, at higher levels of energies [5,10] MeV, the two curves are identical.

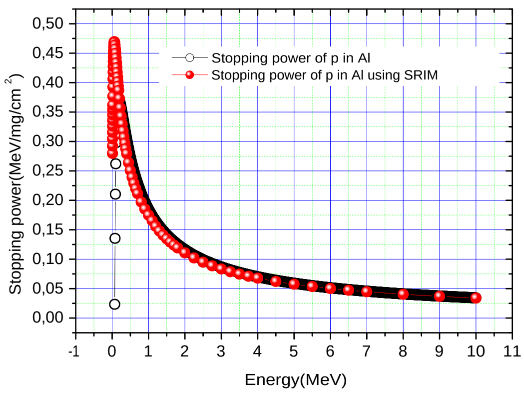

Figure 3.9: Stopping power of proton in Al

The proton stopping power curves show that the maximum divergence between the curve generated by SRIM and that derived from the Bethe-Bloch formula developed using FORTRAN is observed at the point at which these curves reach the higher stopping power value. We notice that this difference is quite small, where it's 0.07 MeV in the curve plotted by SRIM and it's 0.1 MeV in the curve plotted using the FORTRAN code. Nevertheless, these two curves show almost indistinguishable similarities in overall shape and trajectory.

By plotting these curves and after the interpretations, we can see that SRIM is much more accurate in modelling the behaviour of ions in matter because it takes into account the specific properties of the material, such as its density and atomic composition, and can be used for both thin and thick targets. However, due to its considerations of correlations and relativistic factors, SRIM provides more precise outcomes compared to the FORTRAN code.

The sum of electronic and nuclear stopping power gives the following graphs:

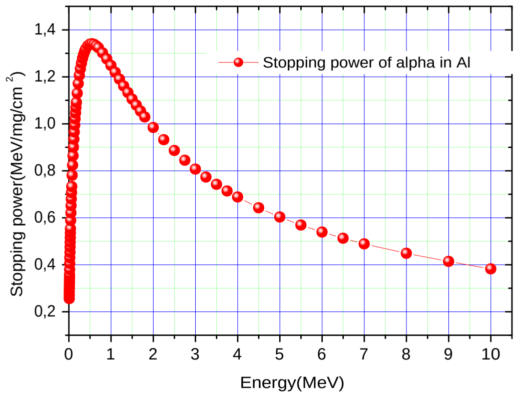

Figure 3.10: Stopping power of alpha in Al with SRIM

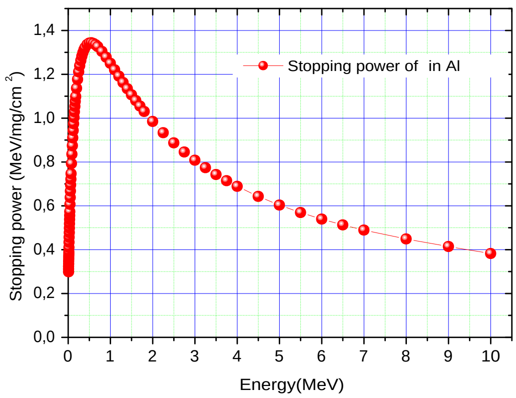

Figure 3.11: Electronic stopping power+Nuclear stopping power of alpha particle in Al

We have noticed that the stopping power curve of aluminium for alpha particles remains unaffected by the addition of nuclear stopping power to electronic stopping power. This observation indicates that the role of nuclear stopping power is not significant and hence can be ignored.

3.6 Range

The range is the distance travelled by the radiation when interacting with matter, which is usually measured in terms of the density of the material through which it passes. This range varies according to a number of factors, including the nature of the radiation (gamma photons, alpha particles, electrons, etc.), the density of the material, its thickness and the composition of the object through which it passes. The range is an important factor in various fields, including radiation protection, nuclear medicine and particle physics. The formula used here is:

$$R(T) = \int_0^t \left[-\frac{dE}{dx}\right]^{-1} dE \tag{3.11}$$

For both α-particles and protons, we have selected an energy that range from 10 keV to 10 MeV.

3.6.1 Range of α-particles

The alpha particle range curve in aluminium represents the distance alpha particles can travel through a layer of aluminium before they lose all their energy. When alpha particles penetrate the aluminium layer, they quickly lose energy because of ionisation and excitation of the atoms in the material. This leads to a decrease in the range of the alpha particles as they get deeper into the material.

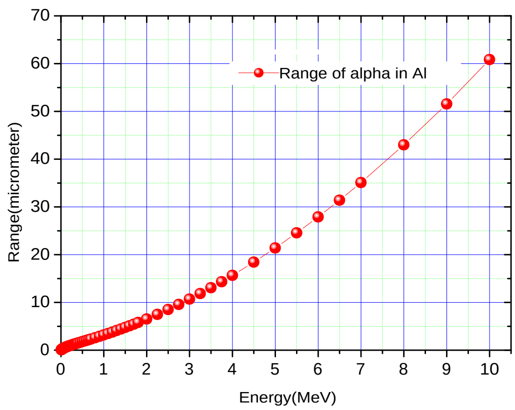

Figure 3.12: Range of alpha particles in Al

This curve shows that the range decreases as the energy of α decreases. At the highest level of energy (10 MeV), the range achieves its maximum which is 60.85 micrometer. At 5.5 MeV, the range fall rapidly to 24.55 micrometer. The range curve at the interval [1,4] MeV decreases more rapidly indicating that α particles are losing more energy and travelling short distances in aluminium. However, when alpha particles lose all their energy (under 1 MeV), the range drops near to 0 micrometer.

3.6.2 Range of protons

The proton range curve in aluminium shows how far protons are able to penetrate aluminium before their energy is lost. This plot illustrates the range of protons in aluminium as a function of their energy.

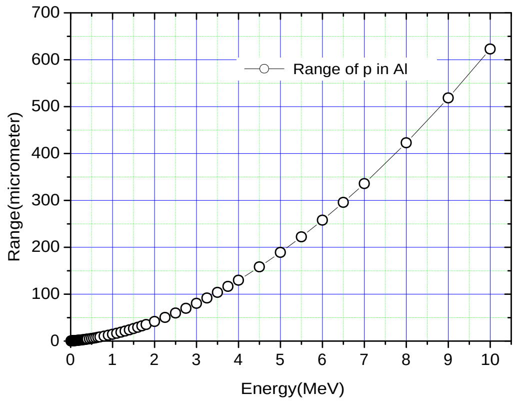

Figure 3.13: Range of proton in Al

At extremely low energies, the range of protons in aluminium is very small, it's almost 0μm. However, as the energy of protons increases, their range also increases. The range curve typically increases with energy until reaching a peak (622.71μm) around 10 MeV. Above 10 MeV, the range begins to decrease. Indeed, at 6 MeV, the range drops quickly to 257.8 μm. From 1 to 5 MeV, the range decreases more than before which means protons are losing more energy and travelling short distances in the aluminium. Under 1 MeV, the range is near to 0 μm because they lose all their energy and stop travelling in aluminium.

Comparison between range curves of alpha and proton in aluminium:

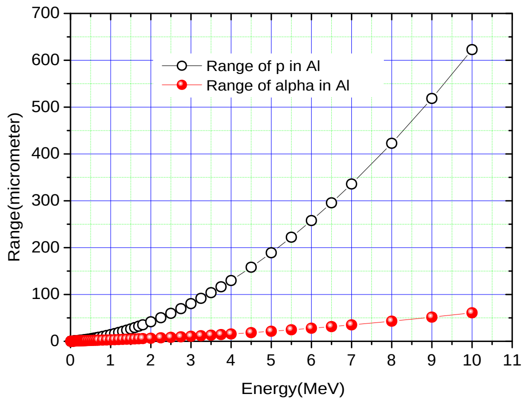

Figure 3.14: Range of alpha and proton in Al

The alpha and proton range curve in aluminium shows how far the particles travel before losing all their energy in the material.
The main reason for the difference in the range curves of alpha particles and protons in aluminium is the fact that alpha particles are heavier and more ionising than protons, and thus lose their energy faster.
In general, the range curve of alpha particles in aluminium is significantly shorter than that for protons, since alpha particles lose the majority of their energy in the first few millimetres of the material. In contrast, protons are able to travel much further before completely losing their energy.
Generally, the range curve of alpha particles in any given material would be shorter than that of protons owing to their higher ionisation power and greater mass. However, this means that they are especially beneficial in applications like cancer therapy, where their capacity to deposit energy in a localised area can be exploited to target and destroy cancer cells.

3.7 Bragg curves

Bragg curves represent graphical plots of the energy deposition of charged particles, like protons, ions and heavy ions, as they pass through matter. The curves illustrate the relationship between the depth of penetration of charged particles into matter and the energy they deposit at each point along their trajectory. Bragg curves are used in radiotherapy, where they allow doctors to precisely target cancerous tissue while minimising damage to healthy tissue.
Here, we used the following equation to plot Bragg curves:

$$-\frac{dE}{dx} = \frac{4\pi e^4 z^2 n Z}{m_e v^2}[ln(\frac{2m_e v^2}{I_{moy}}) - ln\left(1-\beta^2\right) - \beta^2] \tag{3.12}$$

We have taken both protons and alpha particles with an energy of 50 MeV.

3.7.1 Bragg curve of α particles

The α Bragg curve in aluminium shows the relationship between α particle energy deposition and penetration depth into the material.

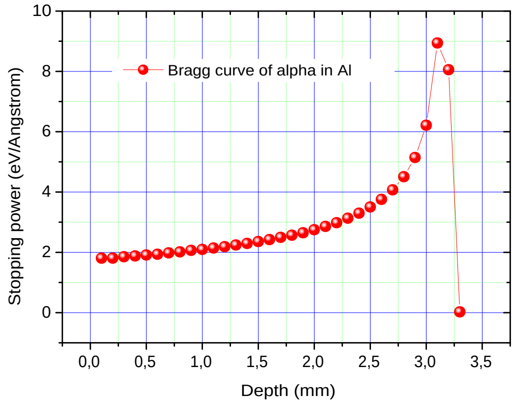

Figure 3.15: Bragg curve of alpha in Al

The plot starts with a sharp increase in energy deposition in the interval [0,3.1]mm until reaching the maximum(8.94 eV/Angstrom) which called Bragg peak. However, as alpha particles move deeper inside the material, their energy disposition decreases until a minimum point(0.02 eV/Angstrom) at 3.3 mm. This decrease happened because α particles keep losing energy until they are completely stopped.

3.7.2 Bragg curve of proton

The Bragg curve of a proton in aluminium is a representation of the energy that the proton deposits as it passes through the material.

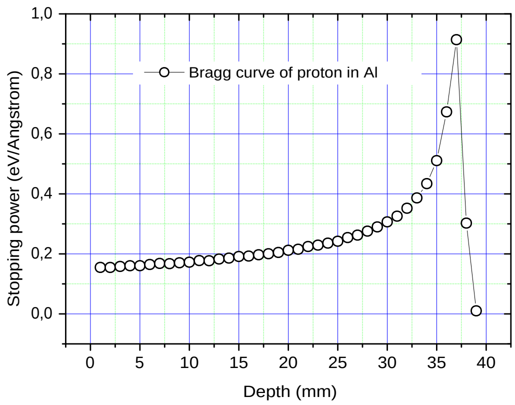

Figure 3.16: Bragg curve of proton in Al

The curve illustrates that the proton loses almost no energy from 0 to 25mm. Above 30 mm, the stopping power starts increasing till reaches the Bragg peak (0.91 eV/Angstrom) at 37 mm where protons lose the most of their energy. Beyond the Bragg peak, the energy deposition decreases rapidly as the proton slows down and eventually stops to reach the minimum point(0.01 eV/Angstrom) at 39 mm.

Comparison between Bragg curves of protons and α particles

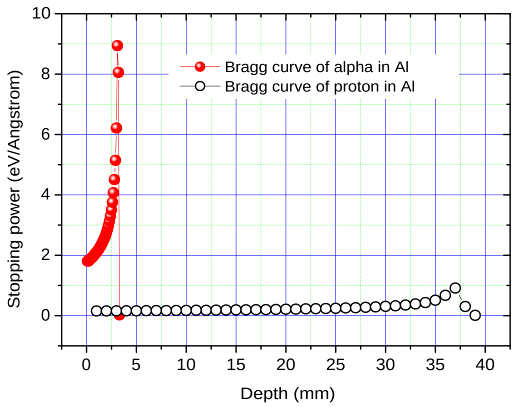

Figure 3.17: Bragg curve of alpha and proton in Al

Alpha particles and protons have separate Bragg curves in aluminium because of differences in mass and charge. α particles are positively charged, heavy particles composed of two protons and two neutrons. These particles have a high ionisation potential and lose energy quickly as they pass through matter. Consequently, the Bragg curve of α particles in aluminium is steep, with energy decreasing rapidly as they travel through the material. The deposition of energy is concentrated near the surface and the α particles stop quickly compared to the protons. In contrast, protons are considerably lighter than α particles and carry a single positive charge. They have a lower ionisation potential and deposit energy more progressively as they travel through matter. The proton Bragg curve in aluminium is steeper and more spread out than that of α particles. The deposit of energy is more uniformly distributed in the material and the protons penetrate further before stopping. To summarise, the Bragg curve of α particles in aluminium is steep and concentrated close to the surface, whereas the proton curve is more spread out and penetrates deeper into the material before stopping. The difference is mainly caused by the differences in mass and charge between the two particles.

3.8 Conclusion

To sum up, in this chapter, we used SRIM simulation code to plot stopping power curves of alpha particles and protons in aluminium, then, compared them to the results obtained from the code which we developed using FORTRAN program. From these curves, we can say that protons stopping power curves are more similar than alpha particles ones. Our exploration utilizing both FORTRAN and SRIM affirms that SRIM proves to be superior in terms of accuracy and precision. This improved accuracy is due to SRIM taking into account a more significant number of interaction mechanisms beyond the classical Bethe-Bloch formula's consideration of ionization and atomic excitation. In addition, SRIM takes into account other factors that influence energy loss and that the classical Bethe-Bloch formula ignores. Using SRIM, we also simulated the range penetration of both protons and alpha particles as travelled aluminium. We have also generated Bragg curves for both protons and α particles in this chapter using TRIM simulation code, followed by a comparison between them.

Chapter 4

Simulation of Stopping Power and Range into Living Tissues

4.1 Introduction

In the previous chapter, we studied the properties and behaviour of charged particles in a given material, and we take aluminium for instance as transport medium. In the present chapter, we will simulate the transport of theses charged particles in living tissues, as an application of the Bethe-Bloch formula in medical physics. A layers model is used to simulate the irradiation of a tumour located in the thyroid gland by means of TRIM simulation code. The TRIM (Transport of Ions in Matter) is a computational sub-module in the SRIM code, introduced and used in the previous chapters. Indeed, by the means of TRIM calculations, it is possible to produce the Bragg peak curve for a given charged particle beam, with a given energy in a given mono/multi- layers medium. several outputs could be obtained, mainly the ionization rate and ions creation within the crossed medium and its layers.

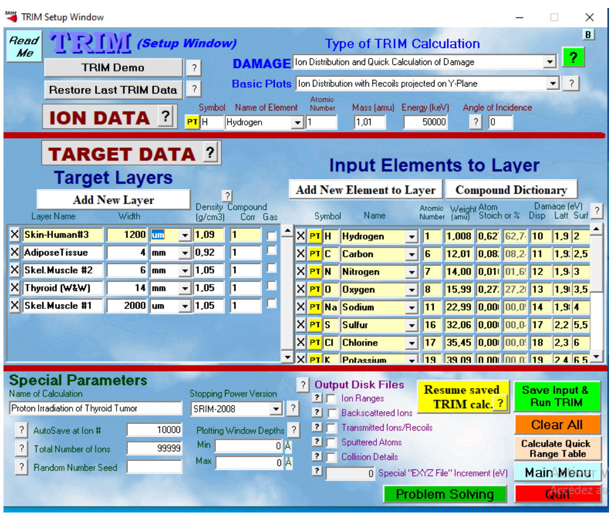

Figure 4.1: TRIM code

4.2 Biological model

To simulate the irradiation of living tissues with charged particles beam, we construct the corresponding geometrical and physical model, based on successive adjacent layers, made from organic matter according to the nature of the tissue. The chemical composition of each layer could be obtained from available tables and already existing materials within TRIM data base.

4.2.1 Geometrical model

In this study, as it is shown in Fig. 4.2, we took the existing thyroid model (W&W), which includes five successive layers:

- The initial layer is the Human Skin#3, with a thickness of 1.2 mm.
- The second layer is the Adipose Tissue, which is 4 mm deep.
- The third layer is the Skeleton Muscle #2, which has a width of 6 mm,
- and the fourth layer is the Thyroid (W&W), with a thickness of 14 mm.
- The final layer is the Skeleton Muscle #2, which has a width of 1.8 mm,

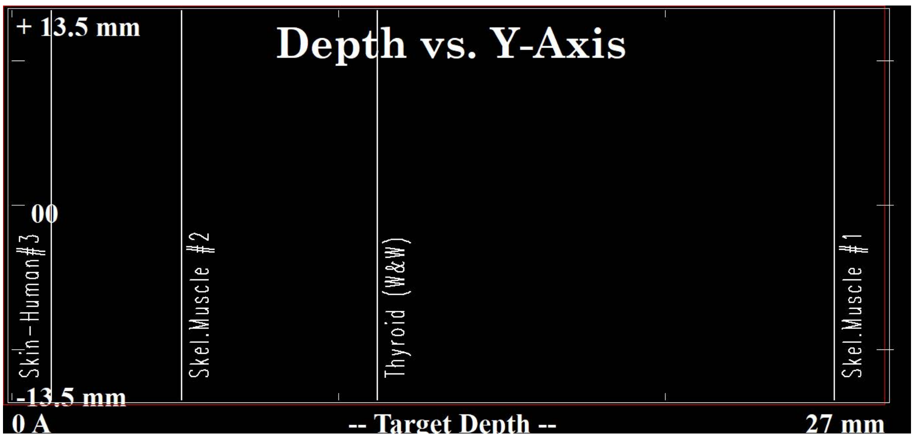

Figure 4.2: Geometrical model

4.2.2 Physical model

Now to fill each layer with its own chemical composition, the existing compounds dictionary allow us to get this composition with corresponding atom fraction of each element, as it could be seen in Table. 4.1 below.

Element	Skin-Human#3 [1.9(g/cm^3)]	Adipose Tissue [0.92(g/cm^3)]	Skel.Muscle #2 [1.05(g/cm^3)]	Thyroid (W&W) [1.05(g/cm^3)]
H	0.62744	0.63482	0.63169	0.6387
C	0.08237	0.28408	0.07432	0.06133
N	0.01654	0.00306	0.01515	0.01061
O	0.27202	0.07775	0.27703	0.28826
Na	0.00054	0.00012	-	0.00054
S	0.00039	-	0.00058	-
Cl	0.00053	0.00018	0.00018	0.00035
K	0.00016	-	0.00064	0.00016
P	-	-	0.0004	-

Table 4.1: Chemical composition of used tissues

4.3 TRIM Simulation

4.3.1 The Effect of Air on Ions

Initially, we carried out a simulation to observe how protons, Helium and Carbon particles with energies of 50 MeV behave in the air and to determine whether they lose a considerable amount of energy before reaching the targeted treatment zone.

Protons

In Fig. 4.3, the obtained curve shows that protons can travel more than 20 metres to reach the Bragg peak limit and they lose totally their energy. This means that protons are able to reach the area to be treated with little loss of energy, even at a distance of 20 metres.

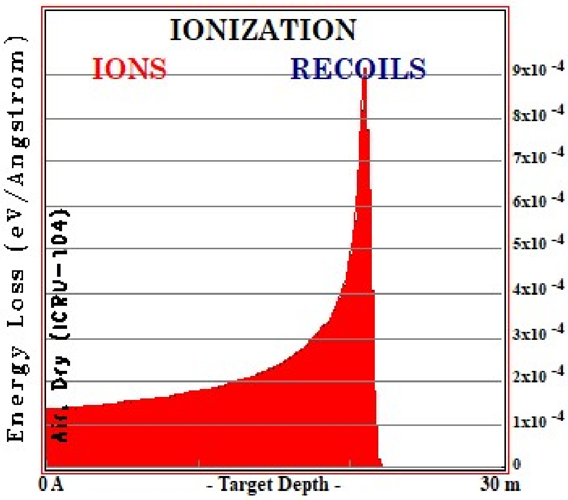

Figure 4.3: Bragg curve of proton in Air

Alpha particle

For the case of Alpha particles, the Fig. 4.4 presents their Bragg curve, in which one can observe that these particles tend to lose the greatest amount of energy around 2 metres. Therefore, if they are within this distance, with an energy of 50 MeV, they can reach their target without losing too much energy.

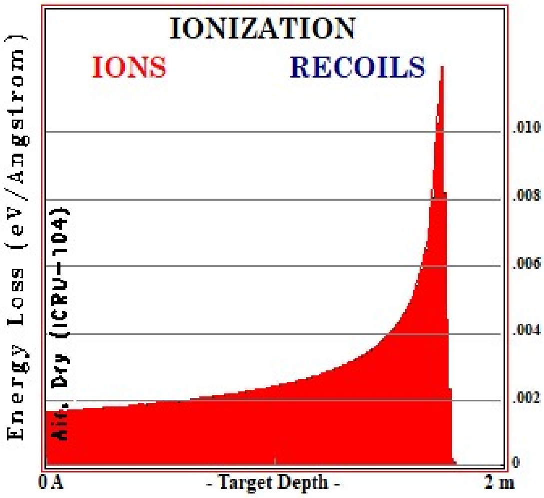

Figure 4.4: Bragg curve of alpha in air

Carbon

In this particular curve, it is clear that the carbon particle will lose the maximum amount of energy after travelling a distance of 11 centimetres. Therefore, in order to reach the desired zone, it would be better for the carbon to be in the close proximity of 0.11 metres. In addition, it should be noted that the energy lost by the carbon particle before reaching the Bragg peak is comparable to the maximum energy lost.

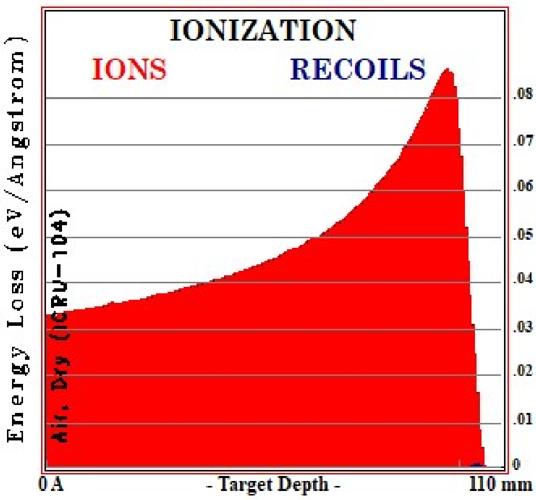

Figure 4.5: Bragg curve of carbon in air

4.3.2 Interaction of Ions with Water

Before beginning the simulation of irradiating the thyroid gland with alpha particles, protons and carbon, we carried out tests on each of these particles with energies of 50 MeV in water to determine their respective penetration levels.

Proton

According to the obtained curve in Fig. 4.6, the energy disposition of protons as they travel in water, stays within a range of $[1, 3] KeV/m$ in the first 20 mm, and the rate will increase considerably in the next few mm to reach the maximal value of 7.5 KeV/m. It indicates that protons lose a small amount of energy (less than 0.1 % of initial energy) when they enter firstly in matter, then they keep loosing energy at the same rate, until they reach the Bragg peak zone where they lose the most of their energy over few mm. The total range of protons in water did not get over 22 mm.

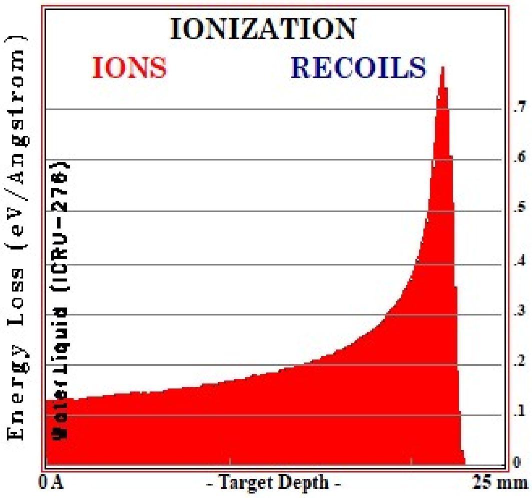

Figure 4.6: Bragg curve of proton in water(50 MeV)

Alpha particles

In the figure below (Fig. 4.7), it can be observed that the alpha particles experience relatively a small rate of energy loss $[15, 40] KeV/m$ through 75% of the traveling range, estimated here to about 1.8 mm. They reach their Bragg peak within 0.1 mm before the range limit.

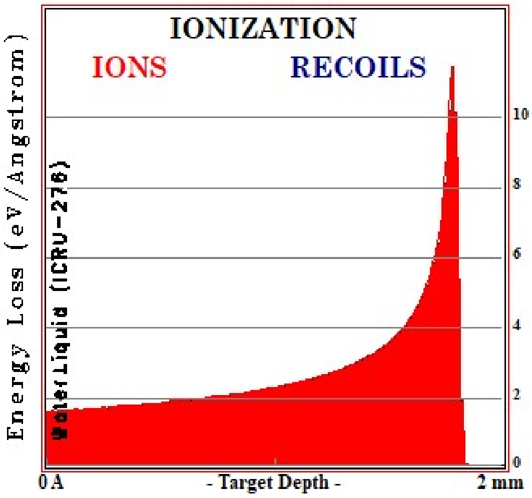

Figure 4.7: Bragg curve of alpha in water(50 MeV)

Carbon

From the plot in Fig. 4.8, it becomes apparent that carbon experiences a significant loss of energy even during the first half of the traveling range. In contrary of both previous particles, carbon ion arrives at the peak after travelling a mere distance of less than 0.01 mm.

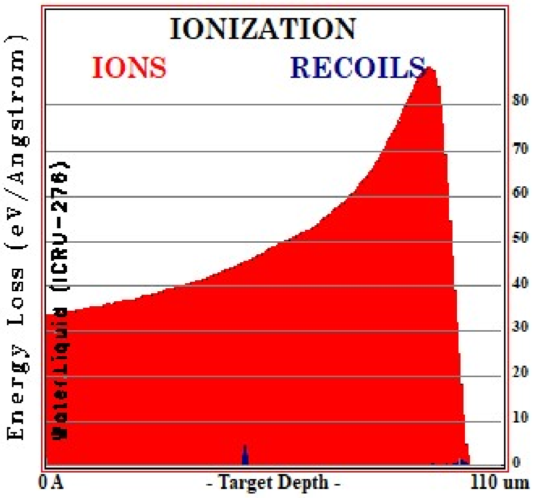

Figure 4.8: Bragg curve of carbon in water (50 MeV)

At the end of this step of simulation, we can conclude that from these three simulated particles, the proton has the highest level of penetration in water. this medium, is the closest one to the living tissues, mainly soft ones. This means that we except that penetration range obtained in the case of water, are very representative and the same range is expected when living tissue model is used.

4.3.3 Thyroid gland

In this part, we tried different energies to find the minimum and maximum energies that the protons, alpha particles and carbon must have to be able to scan all the the thyroid gland depth by tuning the beam energy to define the appropriate energy interval to reach any tumour zone within the organ of interest.

Proton

By varying the protons energy when we simulate the irradiation of the thyroid model, it was possible to determine the minimum and maximum energies for protons to reach the scan the whole thyroid area. Indeed, the protons energy should be within the range [35, 54] MeV, as it could be seen from Fig. 4.9 and Fig. 4.10, respectively.

Bragg curves

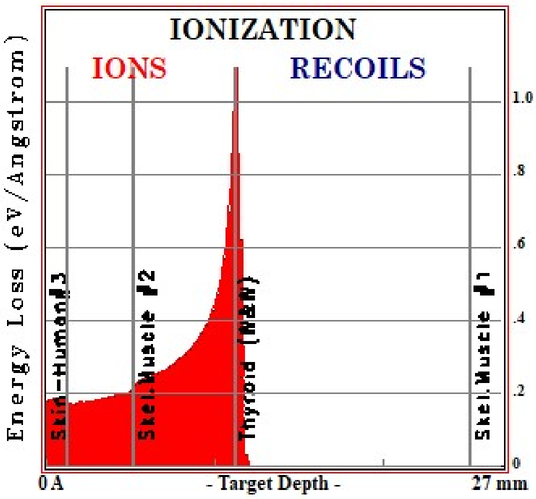

Figure 4.9: Bragg curve of proton in thyroid (35 MeV)

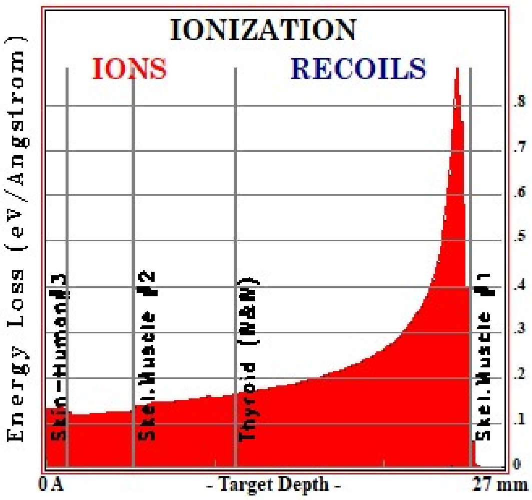

Figure 4.10: Bragg curve of proton in thyroid(54 MeV)

The rate of energy loss in this case, is almost the same registered in the case of the penetration of water. It should be also noticed, that the penetration range is about 25 *mm*, which is about 3 *mm* more than the penetration range found in the case of water.

Damage events

Within the energy range of [35, 54]MeV, protons will provoke collisions as indicated in Fig. 4.11 and Fig. 4.12. The collision rate will range from 80 *colls./mm* (for 35 MeV) to about 60 *colls./mm* (for 54 MeV). indicating that the damage strength will also decrease when the penetration range is increasing. This is very coherent with the energy loss rate, since the most important one is encountered for lowest particles energy, while for higher energy particles, this rate will decrease as ions travel again in the medium. It should be noticed that, under those both limits, the produced collisions are always around 10 *colls./mm* before Bragg peak. This represent a fraction ranging from 12.5 to 15% of induced collisions at Bragg peak.

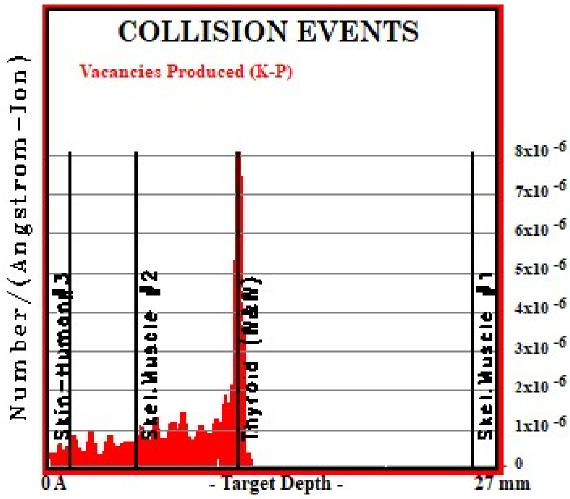

Figure 4.11: Damage events of proton in thyroid (35 MeV)

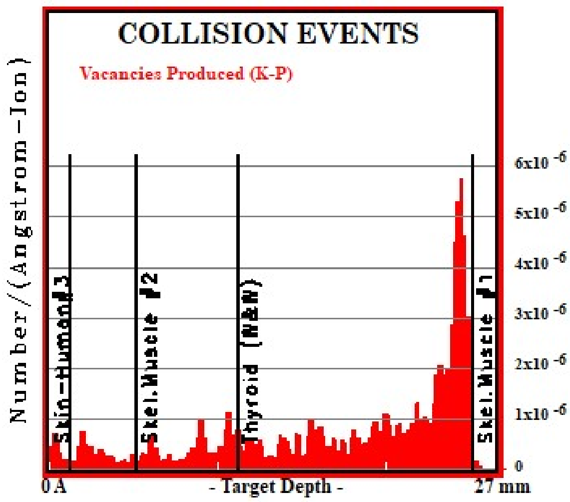

Figure 4.12: Damage events of proton in thyroid(54 MeV)

Alpha particles

Bragg curves

In the case of alpha particles, the energy should range between 140 and 217 MeV (Fig. 4.13 and Fig. 4.14) to scan the thyroid area, to allow any susceptible treatment within this region. We can also observe that the loss rate in both case is varying from 5-10 KeV/m to 42.5-47.5 KeV/m, which stay higher than the protons case.

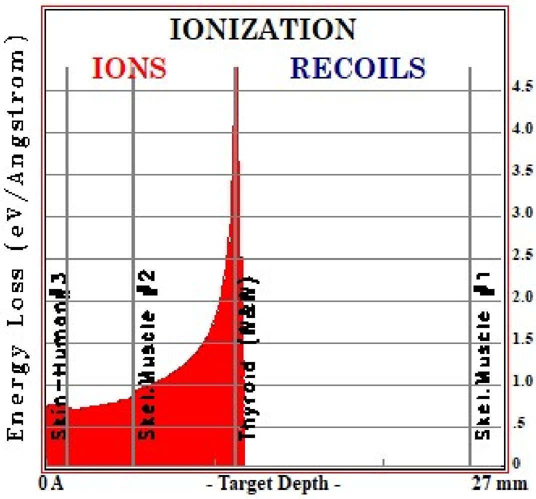

Figure 4.13: Bragg curve of alpha particle in thyroid(140 MeV)

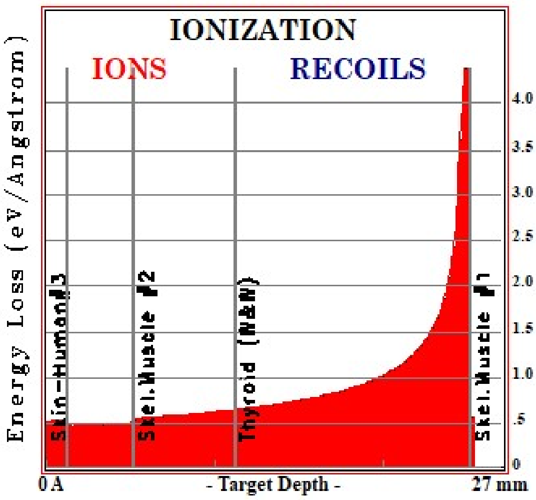

Figure 4.14: Bragg curve of alpha particle in thyroid (217 MeV)

Damage events

At both the minimum and maximum energy levels required for alpha particles to scan the thyroid gland thickness, the registered damage in terms of produced collisions at the same beam intensity, vary from about 430 *colls./mm* (for 140 MeV) to 510 *colls./mm* (for 217 MeV). The ionization effect is about 5 times greater than the protons effect. That indicates that alpha particles are very efficient than protons, but they should be 4 times energetic than protons to reach the zone of interest.

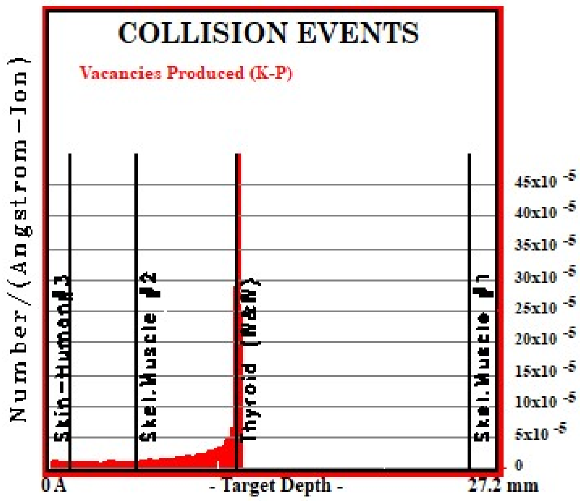

Figure 4.15: Damage events of alpha particle in thyroid (140 MeV)

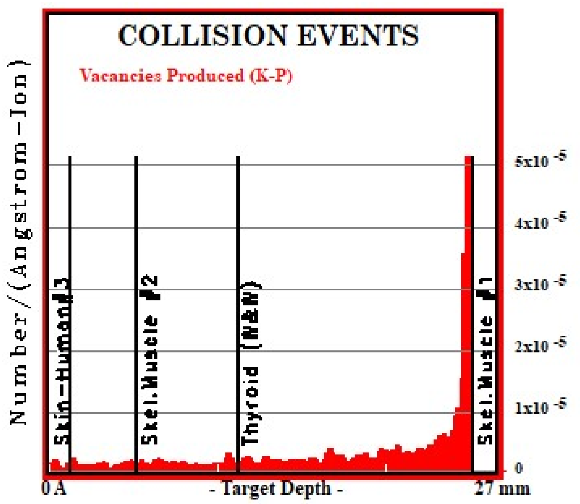

Figure 4.16: Damage events of alpha particle in thyroid (217 MeV)

Carbon

Bragg curves

The minimum energy that carbon needs to enter to the thyroid zone is 760 MeV as it shown in Fig. 4.14. The energy loss rate before reaching the Bragg peak is around 50 KeV/m.

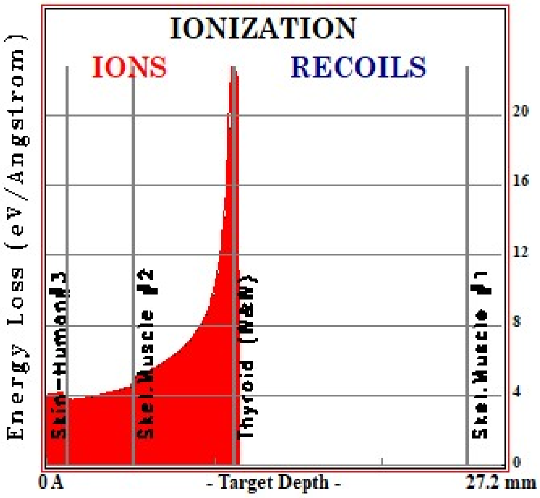

Figure 4.17: Bragg curve of Carbon in thyroid(760 MeV)

The maximum energy for carbon to reach the end of thyroid gland zone occurs at 1.2 GeV. However, the energy loss rate before reaching the Bragg peak surrounding is between 30 and 80 KeV/m, according to Fig. 4.15 below.

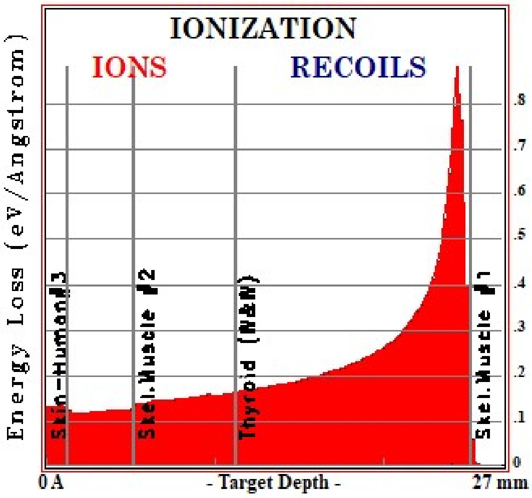

Figure 4.18: Bragg curve of Carbon in thyroid (1.2 GeV)

Damage events

We observed that the damages effected for both minimum and maximum, respectively, range within [4700, 3200]$colls./mm$, which is very important rate of collisions compared to both protons and alpha particles.
While, the penetration range in the case of the three simulated particles, could be reached from minimal energies corresponding respectively to 35 MeV for protons, 140 MeV for alpha, and finally 720 MeV for carbon. While the damage effect could be regulated by varying the beam intensity for each type of ions, the needed power to generate the corresponding beam energies should be drastically increased, when the ions mass increased, to scan the thyroid gland thickness. Consequently, protons present the best choice to reach

the zone of interest by ions irradiation.

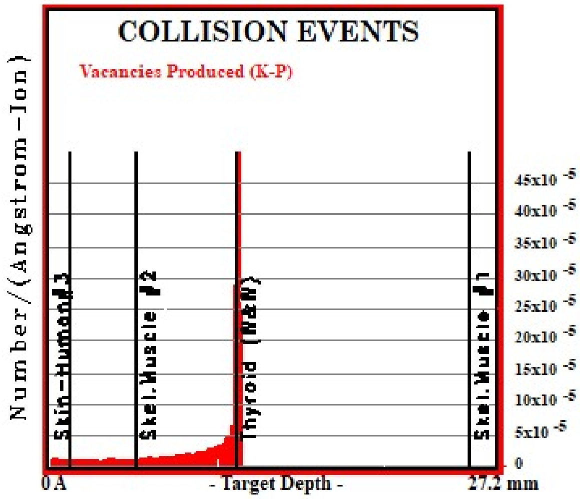

Figure 4.19: Damage events of Carbon in thyroid(760 MeV)

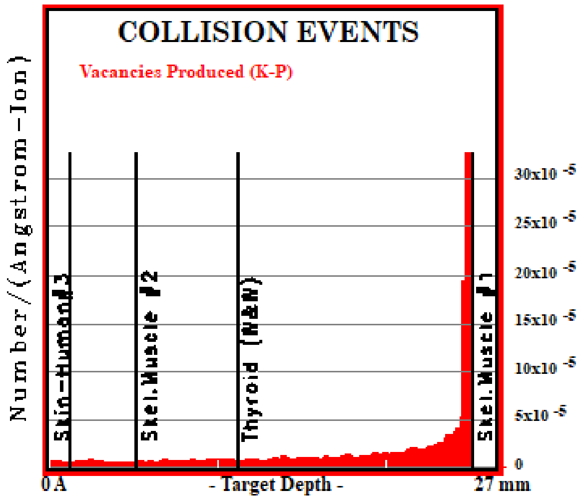

Figure 4.20: Damage events of Carbon in thyroid(1.2 GeV)

4.3.4 Tumour

In this part, we'll conduct a simulation by considering protons to irradiate a tumour located in the middle of thyroid layer.

Bragg curves

To reach the beginning of the tumour, protons must be produced at minimal energy of 46 MeV, with a maximal energy loss rate at 8 KeV/m at the Bragg peak.

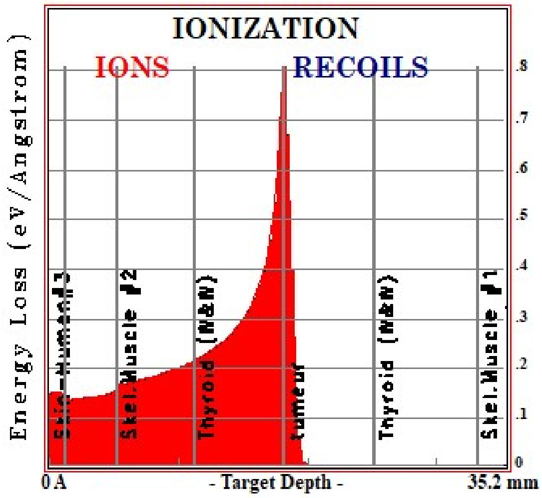

Figure 4.21: Bragg curve of proton in tumour(46 MeV)

To reach the end of tumour thickness, protons must not exceed the energy of 51.8 MeV. The maximal rate of energy loss is about 55 KeV/m.

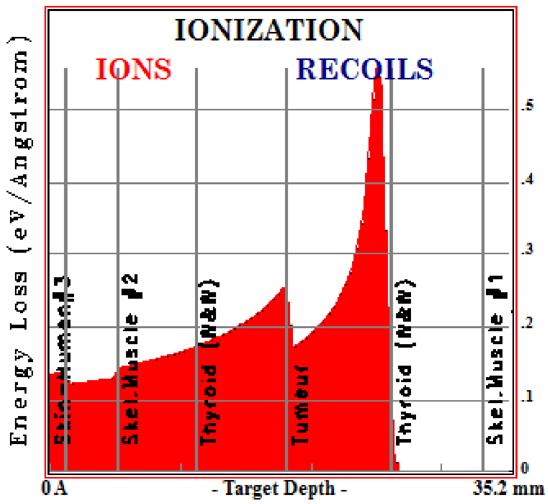

Figure 4.22: Bragg curve of proton in tumour(51.8 MeV)

Damage events

The damages in terms of collisions provoked by each proton passing through the tumour zone, are 4.5 *colls./mm* and 4.2 *colls./mm*, respectively. Meanwhile, the collisions in healthy tissue, did not exceed 2 *colls./mm* for the less energetic beam, while less than 1 *colls./mm* are required for the most energetic one.

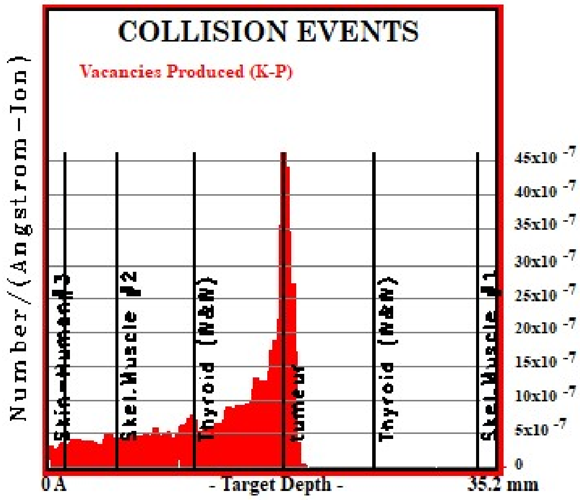

Figure 4.23: Damage events of proton in tumour (46 MeV)

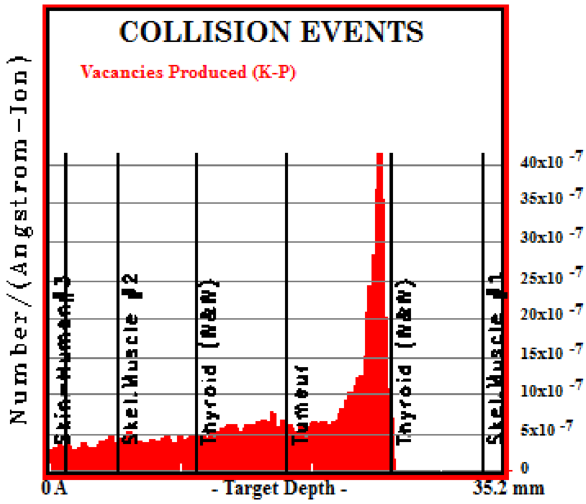

Figure 4.24: Damage events of proton in tumour (51.8 MeV)

4.4 Conclusion

In conclusion, the simulations performed using the TRIM simulation code to study the transport of He, proton and carbon in a thyroid tumour have shown that protons are the best choice for delivering ionising radiation to the desired treatment zone.

General Conclusion

In conclusion, this dissertation presented a comparison between the classical Bethe-Bloch formula developed in FORTRAN and the simulation code SRIM, as well as an application in medicine.
The aim of this study was to evaluate the performance of the two methods for predicting the stopping powers and ranges of heavy ions in different materials, using the stopping powers and ranges of protons and α particles in $^{27}_{13}Al$. Bragg curves were also plotted using TRIM simulation code in order to better understand the behaviour of these particles in aluminium. The results obtained by the two methods were very similar, but there were also some differences.
The FORTRAN program was relatively simple and could be used to calculate the stopping power of protons and α particles in ^{27}Al. However, it did not provide a detailed view of their energy loss distribution within aluminium. In contrast, the SRIM code provided a more detailed analysis of the energy loss distribution, including scattering effects of these particles interacting with the target, making it a more comprehensive tool for simulating the interactions between ions and matter.
Overall, the study showed that the classical Bethe-Bloch formula is a useful for predicting the stopping power of heavy ions interacting with matter, but that SRIM simulations are more accurate and significant due to its ability to provide a detailed energy loss distribution of ions in materials.
In medical applications, protons, alpha particles and carbon are chosen to treat the thyroid. To choose the most appropriate particles to treat a thyroid tumour. Using the TRIM simulation code, we tested these particles on a healthy thyroid to determine the best option for treating thyroid tumours. Our findings indicate that protons have greater penetration and are the most effective for treating thyroid tumours. Additionally, we discovered that α particles can be utilized for surface-level cancers and tumours.
Finally, although the classical Bethe-Bloch formula developed with FORTRAN has been widely used to describe ionising energy loss in materials, it is possible to improve its accuracy by including additional physical effects such as the effects of quantum mechanics and the effects of density functional theory. If we want to compare how electrons and ions behave with matter, we cannot use SRIM and TRIM simulation software because they do not study how electrons interact with matter. However, we can use other codes like GEANT4 and MCNP for this purpose. These software packages can simulate how electrons interact with matter and can help us understand their behaviour better. However, since we were unable to generate range curves and Bragg curves using the classical Bethe-Bloch formula developed with FORTRAN,we can try to use other software programs as MATLAB.

Bibliography

[1] AHMED, Syed Naeem. Physics and engineering of radiation detection. Academic Press, 2007..

[2] LEROY, Claude et RANCOITA, Pier-Giorgio. Principles of radiation interaction in matter and detection. World Scientific, 2011.

[3] KNOLL, Glenn F. Radiation detection and measurement JOHN WILEY &SONS. Inc., New York, 2000, vol. 65.

[4] L'ANNUNZIATA, Michael F. (ed.). Handbook of radioactivity analysis. Academic press, 2012.

[5] CORREA, Alfredo A. Calculating electronic stopping power in materials from first principles. Computational Materials Science, 2018, vol. 150, p. 291-303.

[6] PISKOUNOV, N. Calcul différentiel et intégral, tomes I, II, Moscou, MIR, 1980. QA303P5824)(*).

[7] http://srim.org/

[8] Wang, M., Huang, W. J., Kondev, F. G., Audi, G., & Naimi, S. (2021). The AME 2020 atomic mass evaluation (II). Tables, graphs and references. Chinese Physics C, 45(3), 030003.

[9] Wang, M., Huang, W. J., Kondev, F. G., Audi, G., & Naimi, S. (2021). The AME 2020 atomic mass evaluation (II). Tables, graphs and references. Chinese Physics C, 45(3), 030003.

[10] Valentin, L. (1988). Physique subatomique: noyaux et perticules, 1. Approche elementaire.